

AD-A073 073

PRINCETON UNIV N J DEPT OF ELECTRICAL ENGINEERING F/G 19/1
THE INFLUENCE OF CONTACT AND INTERFACE EFFECTS OF THE ELECTRONI--ETC(U)
JUL 79 P MARK DAAG29-76-G-0017

UNCLASSIFIED

ARO-12606.2-P

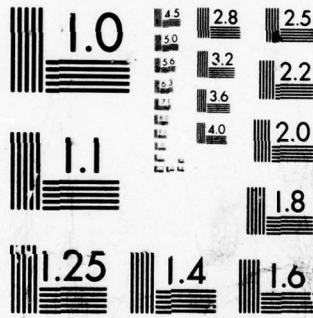
NL

| OF |

AD
A073073



END
DATE
FILMED
9-79
DDC



MICROCOPY RESOLUTION TEST CHART
NATIONAL BUREAU OF STANDARDS-1963-A

REPORT DOCUMENTATION PAGE

READ INSTRUCTIONS BEFORE COMPLETING FORM

1. REPORT NUMBER 19 12606.2-P, 13370.2-P	2. GOVT ACCESSION NO. 18 ARO's ARO's	3. RECIPIENT'S CATALOG NUMBER
4. TITLE (and Subtitle) 6 THE INFLUENCE OF CONTACT AND INTERFACE EFFECTS OF THE ELECTRONIC PROPERTIES AND STABILITY OF CHEMICALLY UNSTABLE MATERIALS		5. TYPE OF REPORT & PERIOD COVERED 9 Final Report 1 Jul 74 - 30 Sep 78
7. AUTHOR(s) 10 Peter/Mark		6. PERFORMING ORG. REPORT NUMBER
9. PERFORMING ORGANIZATION NAME AND ADDRESS Princeton University Department of Electrical Engineering Princeton, New Jersey 08544		8. CONTRACT OR GRANT NUMBER(s) DAHC04 74 G 0193; " 75 G 0085; DAAG29 76 G 0017
11. CONTROLLING OFFICE NAME AND ADDRESS U. S. Army Research Office P. O. Box 12211 Research Triangle Park, NC 27709		10. PROGRAM ELEMENT, PROJECT, TASK AREA & WORK UNIT NUMBERS
14. MONITORING AGENCY NAME & ADDRESS (if different from Controlling Office) 11 23 Jul 79		12. REPORT DATE July 23, 1979
LEVEL II		13. NUMBER OF PAGES 52
		15. SECURITY CLASS. (of this report) Unclassified
		15a. DECLASSIFICATION/DOWNGRADING SCHEDULE

16. DISTRIBUTION STATEMENT (of this Report)
Approved for public release; distribution unlimited.
12 53 p.

DDC
RECEIVED
AUG 24 1979
RECEIVED
C

17. DISTRIBUTION STATEMENT (of the abstract entered in Block 20, if different from Report)
15 ✓ DAAG29-76-G-0017, ✓ DAHC04-74-G-0193

18. SUPPLEMENTARY NOTES
The view, opinions, and/or findings contained in this report are those of the author(s) and should not be construed as an official Department of the Army position, policy, or decision, unless so designated by other documentation.

19. KEY WORDS (Continue on reverse side if necessary and identify by block number)

unstable materials	explosives
chemically unstable materials	azides
electronic properties	
auger electron spectroscopy	

20. ABSTRACT (Continue on reverse side if necessary and identify by block number)

This report summarizes an effort to assess the usefulness of electron beam probe analysis, such as Auger electron spectroscopy (AES), in the analysis of initiation event in primary explosives, principally, azides. Attempts were made to extract a variety of chemical and physical information from AES analyses of KN₃ and NaN₃ crystal specimens to determine whether one could ascribe the chemical instability of these materials to surface as distinct from volume properties.

- 400 734

A 073073
DDC FILE COPY

FINAL TECHNICAL REPORT:

The Influence of Contact and Interface Effects
of the Electronic Properties and Stability
of Chemically Unstable Materials

Grant No. DAAG29-76-G-0017

Prepared by:

Peter Mark, Principal Investigator
Department of Electrical Engineering
Princeton University
Princeton, New Jersey 08544

July 23, 1979

Accession For	
NTIS GRA&I	<input checked="" type="checkbox"/>
DDC TAB	<input type="checkbox"/>
Unannounced	<input type="checkbox"/>
Justification	
By _____	
Distribution/ _____	
Availability Codes	
Dist.	Avail and/or special
A	

79 08 23 038

The major aim of this research effort as stated in the original proposal was to assess the usefulness of electron beam probe analysis, such as Auger electron spectroscopy (AES), in the analysis of initiation event in primary explosives, principally, azides. We attempted to extract a variety of chemical and physical information from AES analyses of KN_3 and NaN_3 crystal specimens to determine whether one could ascribe the chemical instability of these materials to surface as distinct from volume properties. Several detonation experiments¹ performed before this work was begun indicated that azide primary explosives functioned via surface chemical instability and the aim of this research was to pin down just what this mechanism is.

The KN_3 and NaN_3 specimens were selected for analysis because they are less dangerous than the Pb and Ag azides actually used as primary explosives. As the several status reports that were prepared during this research described in detail, the technique of AES was unsatisfactory for this type of analysis. The principal reason for this is that the power density fed to the single crystal specimens by the primary electron beam ($\sim 10^5$ watts/cm³ in a volume 1 mm² by 100Å) was too great to prevent the decomposition of the azide material in the 10^{-10} torr-vacuum range in which the AES analysis is carried out on clean-surface specimens. A second difficulty which we encountered was that the azide materials were generally too insulating to remain at ground potential relative to the electron spectrometer. Several pulse-type techniques were attempted to circumvent this problem, all of them unsuccessful.

Our general experience with these analyses was that the alkalai azide crystals were decomposed by the action of the primary electron beam in a manner that developed an alkalai metal film on top of the azide crystal with the release of nitrogen gas. This alkalai metal film completely passivated the azide material. We were able to establish various interfacial properties (e.g., contact potential) between to alkalai film and the azide substrate, but none of these properties bore significantly on any of the detonation mechanisms we were after. These various efforts are summarized in the status reports.

After two years of effort, we decided that it would serve no useful or justifiable technical or scientific purpose to continue a research effort that was basically unsuccessful. It was at this point (first half of 1977) that we asked for, and received, permission to redirect this work along entirely different lines. Rather than use AES to investigate the surface chemistry of azides, we recommended instead that we apply the technique of Scanning Auger Microscopy (SAM) to the study of wear and erosion of large calibre bore surfaces. The status report where this redirection was suggested is attached as Appendix A. This status report covered the period 7/1/77 to 12/31/77 and describes in detail our reasons for wishing to redirect the nature of the research.

Our initial efforts in the application of SAM analysis to bore surface wear and erosion of specimens obtained from a worn 105 mm tank gun revealed many results that were heretofore not known. These are summarized in the status report covering the period 1/1/78 to 6/30/78,

attached as Appendix B. The principal result is that the bore surface is covered with complex layers of inorganic salts derived from the residues of the propellant constituents and from other items in the breach chamber during firing. In the particular specimen in question, which was obtained from a Cr-plated barrel fired with fixed ammunition in which the propellant was in a Zn-plated steel casing, the principal ingredient of the coating was ZnO. Other salts of Ca, Al, K, P and S were also detected. At the time that this project was terminated and renewed as grant no. DAAG29-79-G-0038, we had not resolved the effects of these deposits on the wear and erosion process. These have since been established in further work under the extension grant as stated in status reports thereunder and at the JANNAF meeting in San Diego, March 1979. A copy of the paper presented at the JANNAF meeting where our initial speculations on wear and erosion mechanisms are given under the renewed grant is attached as Appendix C.

REFERENCES

1. J. Alster, D. S. Downs, T. Gora, Z. Iqbal, P. G. Fox and P. Mark, STABILITY AND THE INITIATION AND PROPAGATION OF REACTION IN THE AZIDES, in ENERGETIC MATERIALS, (Plenum Press, New York, 1977), H. D. Fair and R. F. Walker, eds., Vol. 1, Chap. 9, pp. 449-497.

Appendix A

PROGRESS REPORT

(TWENTY COPIES REQUIRED)

1. ARO PROPOSAL NUMBER: 13370
2. PERIOD COVERED BY REPORT: 7/1/77 - 12/31/77
3. TITLE OF PROPOSAL: THE INFLUENCE OF CONTACT AND INTERFACE EFFECTS ON THE ELECTRONIC PROPERTIES AND STABILITY OF CHEMICALLY UNSTABLE MATERIALS
4. CONTRACT OR GRANT NUMBER: DAAG26-76-G-0017
Department of Electrical Engineering
Princeton University
5. NAME OF INSTITUTION: _____
6. AUTHOR(S) OF REPORT: Peter Mark, Professor of Electrical Engineering
Principal Investigator
7. LIST OF MANUSCRIPTS SUBMITTED OR PUBLISHED UNDER ARO SPONSORSHIP DURING THIS PERIOD, INCLUDING JOURNAL REFERENCES:
8. SCIENTIFIC PERSONNEL SUPPORTED BY THIS PROJECT AND DEGREES AWARDED DURING THIS REPORTING PERIOD:
J. L. Yeh, graduate student, half time
E. So, graduate student, half time
A. Amith, research associate, one-third time.

14710-EL

Dr. Peter Mark
Princeton University
Department of Electrical Engineering
Princeton, NJ 08540

BRIEF OUTLINE OF RESEARCH FINDINGS

We have been continuing to assess the applicability of electron beam probe analysis, principally Auger electron spectroscopy (AES) to the study of the surface properties of chemically unstable materials, specifically KN_3 and NaN_3 . We have now reached the conclusion that surface diagnostics with electron beam probes are unsuited to these materials. The underlying reason is that the input of such high energy densities (10^5 watts/cm³ for primary beam voltages and currents, ~ 1 kV and ~ 1 μ A, respectively, for typical AES analyses) invariably causes instantaneous decomposition of the azide material. All attempts at reducing the average input power, e.g., by using pulse techniques and phase sensitive detection, have been unsuccessful in preventing surface decomposition. Although it might be of scientific interest to study the properties of alkali metal film on azide materials formed by the electron beam-induced decomposition of the azide, we have reached the conclusion that such a study would not fulfill the stated objectives of this research. Instead, we have decided to request that we be permitted to redirect this work into an area that is of equal, if not greater importance to the Army and that is demonstrably well suited for investigation with existing and newly acquired research instrumentation. We refer to the study of gun barrel wear and erosion using scanning Auger electron spectroscopy to study grain boundary metallurgy, and ion erosion Auger electron spectroscopy for compositional depth profile analysis. The remainder of this status report serves as a "mini proposal" for the re-direction of this research.

Gun barrel wear and erosion is the consequence of a complicated interplay of several factors that provide a most unusual environment at the surface and near surface of the gun barrel bore during firing.¹

- 1) Transient high temperature ($\sim 2000^\circ\text{K}$) and high pressure (up to 80,000 psi).
- 2) Chemical interactions between the propellant gases and additives and the bore surface.
- 3) Mechanical and metallurgical interactions from the rotating bands and particulate matters from the propellant. Many empirical methods have been developed to reduce adverse consequences of this catastrophic environment in the metallurgy of the barrel, the

composition of the propellant charge and the structure of the rotating band. Specifically, the bore surface temperature can apparently be lowered by the incorporation of ablators² and wear-reducing additives (wax and titania-wax combinations)³ and low flame temperature propellants.⁴ Stress and temperature enhanced bore corrosion have also been reduced through the development of propellants with less corrosive gaseous products. Gun barrel liners and metallurgical coatings have also been developed to reduce the combined adverse effects of thermal and pressure transients and exposure to corrosive gases.¹ The adverse effects of copper deposition from the rotating bands have been reduced by the incorporation of lead foils into the propellant charge as a decoppering agent⁵ and by the use of plastic rotating bands.¹ However, none of these adhoc approaches have reliably reduced gun barrel wear and erosion to acceptably low levels. More important, there exists no basic understanding of these various adverse effects.¹

The following technical questions can be posed to achieve an understanding and better control of wear and erosion effects.⁶ 1) What is the physical and chemical state of material removed from the barrel surface? 2) What is the removal rate? 3) What combination of mechanical, chemical, physical and thermal processes lead to removal of material? 4) What is the composition (and, it might be added, structure) of the bore surface after firing?

The research proposed here addresses primarily the last of these items, although it intersects with the others. It is proposed to apply the techniques of Auger electron spectroscopy (AES) to the study of the bore surface metallurgy in an effort to determine the compositional and structural changes at the bore surface caused by normal firing. The polycrystalline and alloy nature of the bore surface can cause redistribution of alloy constituents without changing over-all alloy composition. The reactive propellant gases can deposit corrosive impurities (e.g., sulfur), leading to stress induced corrosion and cracking. Unknown impurities present in trace amounts at intergrain boundaries can also contribute to temperature, pressure and chemically induced corrosion and wear.⁷ Finally, as significant loss of material occurs from the inside of a gun barrel, and also because metallurgical coatings are frequently recommended to reduce the effects of wear and corrossions, it is important

to study the composition and structure of the interface between the damaged and undamaged portions of the barrel, and the interface between the barrel coating and the substrate. In the latter case, this is important because of differential thermal stresses that can appear at this interface. To address the questions, it is proposed that Auger electron spectroscopy (AES) analyses be conducted in the scanning mode, using a scanning Auger microprobe (SAM) with about 1 micron resolution, coupled with ion erosion and low temperature fracturing to allow depth-profiling analyses.⁸

Among the various bore surface problems important to gun barrel erosion, there are two that appear to lend themselves particularly well to SAM analyses. These are both metallurgical in nature: 1) The study of the effect of firing on the free bore surface; specifically on the grain structure, alloy component distribution, chemical product formation of propellant reactions with the bore metal, and the formation of stress and chemically induced cracks. 2) The study of metallurgical coating used to reduce wear such as chromium and nickel alloy component distributions, the effect of other impurities, such as carbon and phosphorous on the wear life, the effect of redistribution of alloy components at grain boundaries, the effect of the copper from the rotating bands and of decoppering agents, the formation and depth distribution of cracks in the coating owing to differential thermal expansion and the study of the coating-substrate interface.

It is planned in the proposed research to study several features of metallurgical changes that can occur at the bore surface during firing. First, the changes in the grain structure will be examined to determine whether the drastic thermal, pressure and chemical environment during firing influence grain size (through melting and recrystallization) and grain boundary composition (through fractional freezing and through the temperature gradients generated during firing). This will be a comparative study where the bore surface is examined with SAM erosion analysis prior and subsequent to firing. The effect of wear reducing additives can similarly be studied by examining the profile and areally resolved distribution of such additives, particularly the inorganic components such as Ti (in TiO_2), Mg and Si (in talc), Mo (in MoO_3) and Ca (in $CaCO_3$).⁹ It would be very useful indeed to observe where these potential impurities

ultimately reside after they have served their thermal shielding purposes during firing and whether they then can contribute adversely to embrittlement after firing. As an extension of the ESCA analyses,¹⁰ which have revealed that corrosive chemical reactions involving propellant gases can continue for days after a firing, it is proposed to examine via the SAM technique where this chemistry occurs. In all likelihood, these extensive chemical reactions are also grain boundary effects that might be inhibited with the incorporation of getter impurities.

Fracture studies of bore specimens can reveal the nature of embrittlement before it has progressed to the stage where massive barrel failure occurs. Here it is proposed that the effect of thermal, pressure and chemical environment on embrittlement be examined to observe the influence of grain boundary contamination.

The use of coatings of refractory metals such as chromium has been recommended as wear reducing agents.^{1,6} However, cracking has been observed owing to differential thermal effects.^{1,6} In particular, the method of deposition of the Cr coating, by CVD, electroplating, and chemical diffusion techniques strongly affect the properties of the coating. The SAM profiling and fracture technique can be used to examine the composition of the coating, especially its gradient near the surface and near the coating-substrate interface. The adhesion of the coating and the effect of differential thermal expansion are determined to a large extent by the interfacial structure and composition. At present, there is no information available on that subject. As a final example, the metallurgical effect of the copper rotating bands on the bore surface can be examined. Little, if anything, is known about the effects of residual copper on the bore surface. It would be constructive to examine the effect of Cu impurities in the grain boundaries on the metallurgy of the bore material. Further, the effect of the lead decoppering agent should be examined, especially on Cr-coated bores as it is known that Cr dissolves in Pb at elevated temperatures. In fact, such solutions are used in the diffusion coating of Cr onto steel to form stainless coatings. It is possible that the very material that is used to remove Cu also might remove the Cr wear resistant coating.

These are only selected examples of the wear and erosion problems that can be addressed with the SAM technique. Clearly, because of its sensitivity to structure and composition, and because of its areal resolution and profiling capability, the SAM technique has many applications beyond the limited examples given above.

The apparatus that is planned for this research comprises a 3 micron resolution SAM system provided with a low temperature fracture mechanism. The SAM unit is a cylindrical mirror analyzer (CMA) electron spectrometer that can be operated either to collect all secondaries (SEM mode) or to collect only the Auger electrons (SAM mode). In either case the primary electron beam is raster-scanned over the specimen surface and the electron spectrometer output is displayed on a kinescope synchronously with the scanning beam to provide area resolution. The vacuum system is also supplied with an argon ion sputtering gun, also capable of being raster scanned over the surface, and a 6-channel multiplexer for the simultaneous profil analyses of 6 elemental species. The purpose of the low temperature fracturing unit is to study embrittlement through the preparation of fractured surfaces whose faces can similarly be examined by SEM and SAM analyses in situ.

The best method for sample preparation for the analyses described in the previous paragraph appears to be a wear sensor. This instrument positions a removable surface element between adjacent land areas of the barrel rifling. The probe surface position can be accurately aligned to be flush with the barrel bore wall. After a firing, the probe can be removed and analyzed by the various techniques just described. Presently, this probe is examined primarily through visual analysis of certain calibrated pre-inscribed surface features (called knoops) before and after a firing. It should be possible to use the same sensor for modern surface analyses.¹¹ For example, the probe surface can be extracted and examined for changes in surface grain structure and intergrain composition. The probe can also be coated with various refractor metals, using various coating techniques and then similarly examined. The probe can also be examined after various propellant with various additives having been fired to test the effects of these variables. The probe can also be fractured to lay bare a plane perpendicular to the probe surface to examine compositional and structural gradients away from the bore surface.

Finally, the effects of different rotating band materials can similarly be examined with this probe. It is anticipated that significant information about the interaction of the firing environment and the bore surface can be anticipated from this analytical scheme.

REFERENCES

1. I. Ahmed, Proceedings of the Tri-Service Gun Tube Wear and Erosion Symposium, Picatinny Arsenal, Dover, New Jersey, March 1977.
2. Brown, et al., Tech. Report AFATL TR-71-164, Dec. 1971.
3. S. Y. Ek and D. E. Jacobsen, U. S. Patent 3148620, Sept. 1966.
4. J. F. Picard and R. Trask, Proceedings of the Tri-Service Technical Meeting on Gun Tube Erosion and Control, Watervliet Arsenal, Watervliet, New York, February 1970.
5. E. Wurzel, Ref. 1.
6. J. R. Ward, Ref. 1.
7. D. F. Stein, J. Vac. Sci. Technol. 12, 268 (1975).
8. A. Joshi, L. E. Davis and P. Palmberg, in Methods of Surface Analysis, (Elsevier, New York, 1975).
9. R. Fedyna, M. E. Levy and L. Stiefel, Ref. 1.
10. Arrangements have been made with Dr. J. Sharma of Picatinny Arsenal to coordinate our AES studies with his ESCA analyses.
11. Arrangements are being made through Dr. Sharma to acquire such specimens.

Appendix B

PROGRESS REPORT

(TWENTY COPIES REQUIRED)

RETAIN THIS COPY

USE JOB NO. _____
• TO CHECK YOUR BILLS
• FOR ALL SERVICES

JUL 31 1978

JOB NO. 587-79
No. Copies 20x40

PRINCETON UNIVERSITY
F. MARK RESEARCH SECTION

1. ARO PROPOSAL NUMBER: 13370
2. PERIOD COVERED BY REPORT: 1/1/78 - 6/30/78
3. TITLE OF PROPOSAL: THE EMBRITTLEMENT OF ALLOYS UNDER IMPULSE THERMAL,
PRESSURE AND CHEMICAL CONDITIONS*
4. CONTRACT OR GRANT NUMBER: DAAG26-76-G-0017
5. NAME OF INSTITUTION: Department of Electrical Engineering
Princeton University
6. AUTHOR(S) OF REPORT: Peter Mark, Professor of Electrical Engineering
Principal Investigator
7. LIST OF MANUSCRIPTS SUBMITTED OR PUBLISHED UNDER ARO SPONSORSHIP
DURING THIS PERIOD, INCLUDING JOURNAL REFERENCES:

8. SCIENTIFIC PERSONNEL SUPPORTED BY THIS PROJECT AND DEGREES AWARDED
DURING THIS REPORTING PERIOD:

J. L. Yeh, graduate student, half time.
E. So, graduate student, half time.
Dr. A. Amith, research associate, one-third time.

* Formally: THE INFLUENCE OF CONTACT AND INTERFACE EFFECTS ON THE
ELECTRICAL PROPERTIES AND STABILITY OF CHEMICALLY UNSTABLE
MATERIALS

13370-P

Dr. Peter Mark
Princeton University
School of Engineering
and Applied Science
Princeton, NJ 08540

BRIEF OUTLINE OF RESEARCH FINDINGS

INTRODUCTION

Following the decision to redirect this research effort to a metallurgical examination of embrittlement effects occurring at bore surfaces,¹ we have begun to examine worn surfaces with SEM/SAM (scanning electron microscope/scanning Auger microprobe) techniques and report here our initial results. Our purpose in the initial stages of this investigation is to determine whether the SEM/SAM technique is capable of resolving important grain boundary segregation and deposition effects at an eroded bore surface, and of yielding useful information about the tenacity of the chromium layer of Cr-coated bore surfaces. Accordingly, we have examined three specimens sectioned from worn bore surfaces: two specimens of a pebbled surface of uncoated gun steel and one specimen of a Cr-coated worn bore surface. For the pebbled surface, we can report that we detected preferential deposition of a TiO₂ wear-reducing additive from the propellant charge at the austenitic grain boundaries, and of a nitrogen-containing compound deep below the bore surface along surface cracks. For the Cr-coated surfaces, we have observed a tenacious ZnO coating on the spent surface, presumably a residue derived from the brass propellant cartridge casings used in this bore.

PEBBLED SURFACE

The pebbled surface specimens (and the Cr-coated specimen) were obtained from Dr. I. Ahmed, Benet Laboratory, Watervliet Arsenal. They were sectioned from a 5-inch naval gun. Two profile aspects of this specimen were examined: normal incidence and tangential incidence. For the normal incidence aspect, the primary electron beam of the cylindrical mirror analyzer (CMA) electron spectrometer was at normal incidence to the pebbled bore surface. An SEM image of the normal incidence aspect, obtained with the CMA operating in the secondary emission mode, is shown in panel a of Fig. 2 (see below). The SAM analysis then determined the areally resolved elemental constituents in the vertical grain boundary shown in the SEM photograph (see remaining photographs of Fig. 2 and discussion below). For the tangential incidence aspect, the primary electron beam was incident normally onto the section cut perpendicular to the pebbled surface. An SEM image of this aspect is shown in panel a of Fig. 6. As this photograph shows, there are rather deep cracks extending from the pebbled surface into the bore. Our SAM analysis determined the elemental constituents in and around these cracks.

1. Normal Incidence Analysis

An Auger electron spectroscopy (AES) trace of a virgin pebbled surface (washed in methanol) is shown by trace a of Fig. 1. The predominance of carbon and oxygen signals is typical of any virgin surface. These elements represent the residues of organic surface contaminants that have been cracked by the 3kV primary electron beam of the CMA. The presence of chlorine and sulfur is also frequently observed on virgin surfaces as environmental contaminants. The small size of the low voltage (47V) iron signal is also evidence of a surface contamination coating. The escape depth of these low energy electrons is of the order of 7Å so that they are easily absorbed by very thin contamination layers. The small Ni and Cu signals are not unusual for a steel surface. The Na and Ti are unexplained at this point in the analysis.

After 8 minutes sputtering with 1kV argon ions, the AES trace b of Fig. 1 was recorded with the primary electron beam incident at point A of the SEM photograph, panel a, Fig. 2. Sputtering has removed the major contaminants. The oxygen signal has been reduced, the carbon signal has been converted, at least in part, to a carbide signature typified by the doublet structure (circled on trace b) on the low energy side of the major 272V peak. The typical iron structure near 700V has come up and the low-voltage 47V iron peak has become much larger signifying that the surface contaminant overlayer has been removed. The Na and Cu peaks are gone indicating that these were contaminants and the Ar-signal from the implanted argon is evident. Most interesting is the continued presence of the Ti-signal.

The photographs of Fig. 2 show the results of the SEM/SAM analysis in the vicinity of the grain boundary shown in the SEM photograph of panel a. Point A of this region is reproduced by the SEM photograph, panel b, at higher magnification. The remaining photographs are SAM images of the 272V C-signal (panel c), the 652V Fe-signal (panel d), the 387V Ti-signal (panel e) and the 514V O-signal (panel f). Panel d shows clearly that the iron signal is obscured by some contaminants at the grain boundaries. Panel e shows that carbon is preferentially present in the grain boundaries but also partially obscured by other constituents and that carbon is also present as a contaminant on the grain surface (vis: bright region at the bottom of panel c which correlates with the dark region on the Fe-image, panel d, and with the dark shading in the SEM image, panel b). In all likelihood, the carbon

Pebbled Surface
AES traces

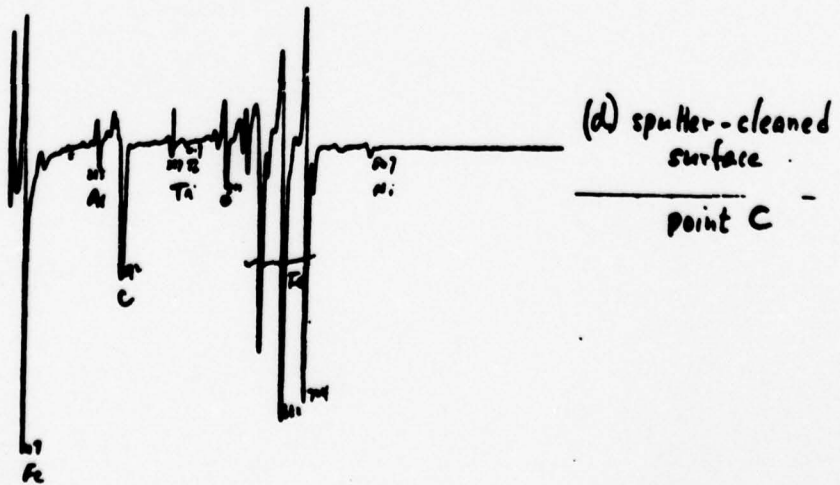
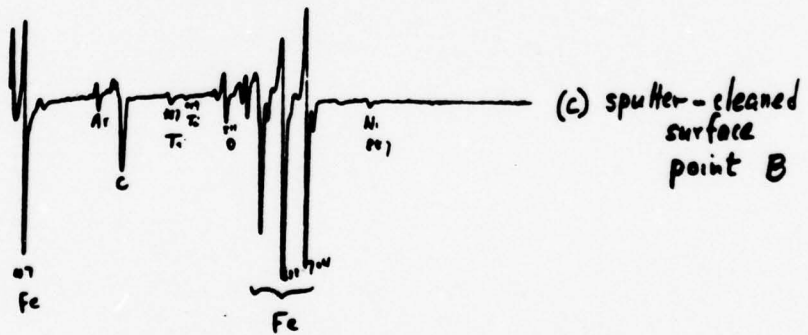
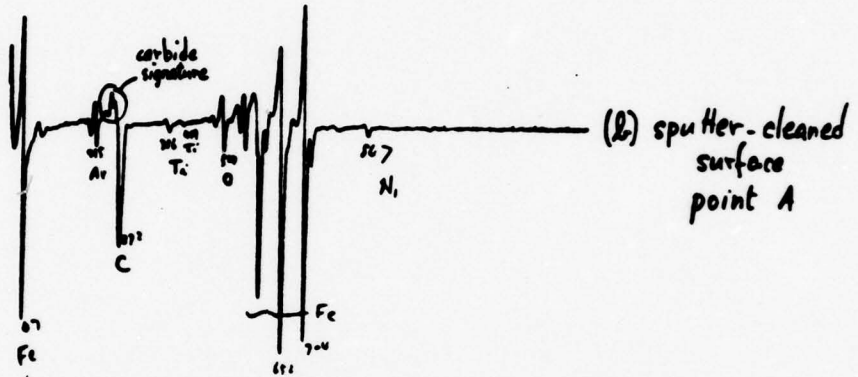
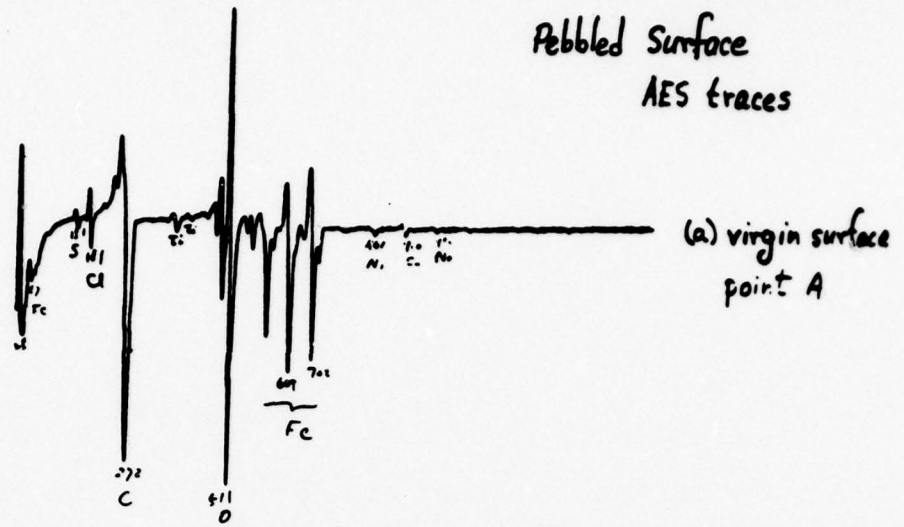
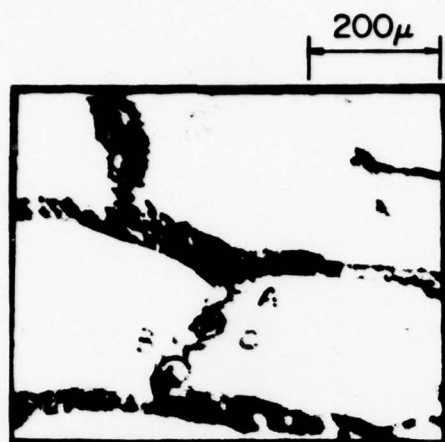
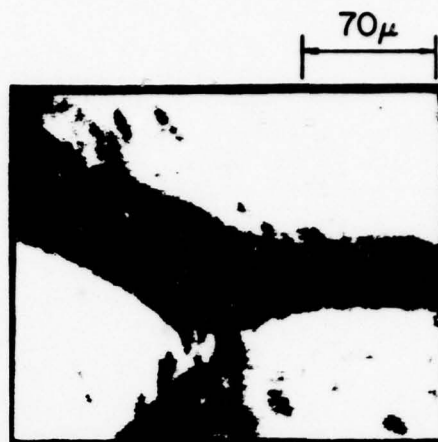


Figure 1

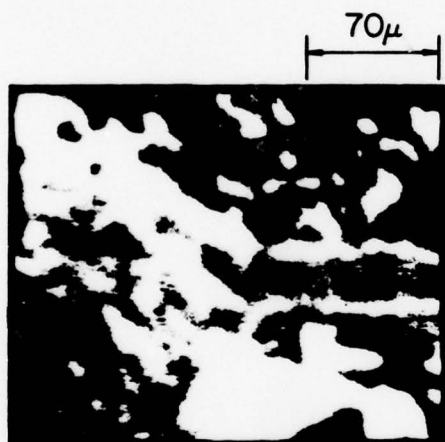
SEM/SAM ANALYSIS: PEBBLED SURFACE-NORMAL INCIDENCE ASPECT



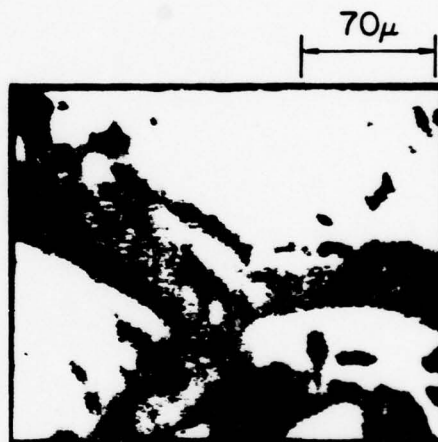
a) SEM IMAGE



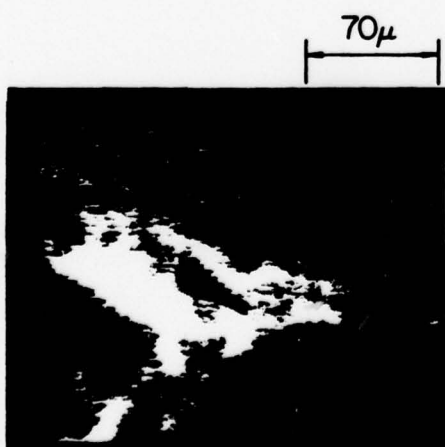
b) SEM IMAGE-POINT A



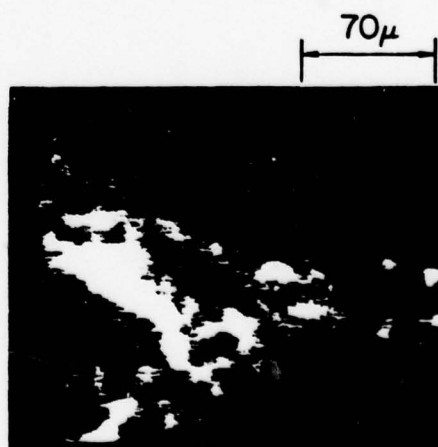
c) C-IMAGE 272 V



d) Fe-IMAGE 652 V



e) Ti- IMAGE 387 V



f) O-IMAGE 514 V

FIGURE 2

in the grain boundaries comprises the carbide portion of the AES signal (Fig. 1) and the carbon deposits on the grain surfaces stem from the propellant. Panels e and f are the Ti- and O-images, respectively. These correlate extremely well and very probably comprise residues from the TiO_2 wear-reducing additive used in at least some of the propellant charges fired in this barrel. The SAM analysis shows that these deposits are strongly preferential at the austenitic grain boundaries. The relative strengths of the Ti- and O-signals of the clean-surface AES traces of Fig. 1 (all but trace a), corrected for Auger emission yields, support this interpretation.

The AES trace c of Fig. 1 was recorded at point B (panel a, Fig. 2) and is essentially identical with trace a. The photographs of Fig. 3 comprise the SEM/SAM analysis of the vicinity of point B. Panel a, is the SEM photograph, showing the secondary emission topography. The remaining panels are SAM images of the Fe-(b), C-(c), Ti-(d), and O-(e) signals. Here too, there is good anti-correlation of the Fe- and O-images and good correlation between the Ti- and O-images.

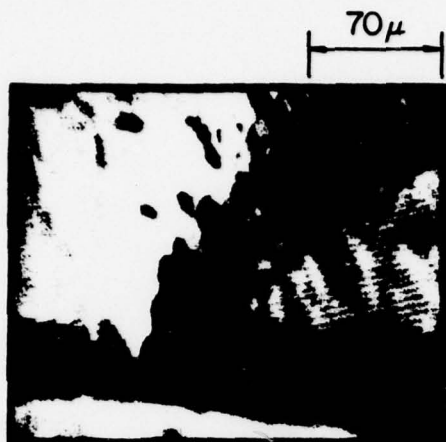
The AES trace d of Fig. 1 was recorded at point C (panel a, Fig. 2). It is also essentially identical with the other clean-surface traces. The photographs of Fig. 4, arranged in the same sequence as those of Fig. 3, comprise the results of the SEM/SAM analysis at point C and show the same anti-correlations of Fe and C, and the same correlations of Ti and O.

From this preliminary analysis we may certainly conclude that traces of the TiO_2 wear-reducing additive remain bound to the bore surface and that the TiO_2 is preferentially deposited at the austenitic grain boundaries. To the author's knowledge the latter fact is new. We may also conclude that carbides are observed in the grain boundaries, a rather well-known phenomenon in steel embrittlement.²

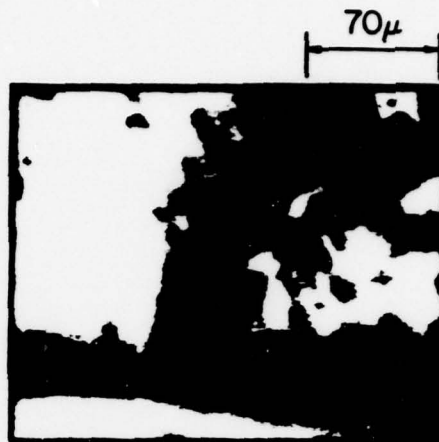
2. Tangential Incidence Analysis

The photograph of Fig. 6, panel a, shows the low magnification SEM image of three cracks (labelled A, B and C) running into the bore surface. This is shown by the tapered dark images running from the wide ends at the pebbled surface to the left into the bore material. The surface containing the cracks was machine-cut. Fractured surfaces will be studied later. The AES traces a, b and c of Fig. 5 were recorded with the primary electron beam incident at the surface-end (wide-end) of cracks A, B and C, respectively.

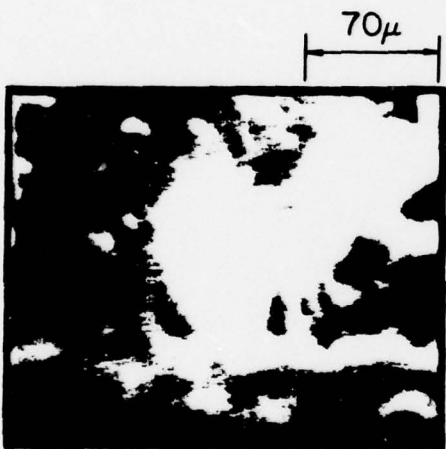
SEM/SAM ANALYSIS: PEBBLED SURFACE-NORMAL INCIDENCE ASPECT



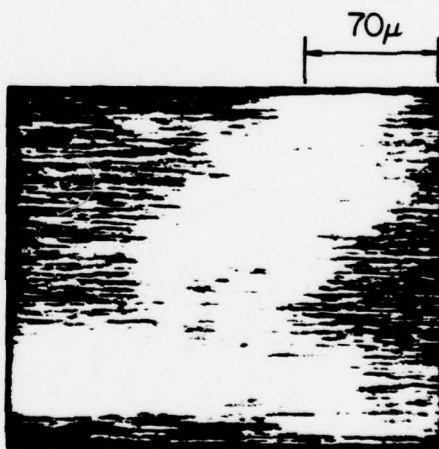
a) SEM IMAGE - POINT B



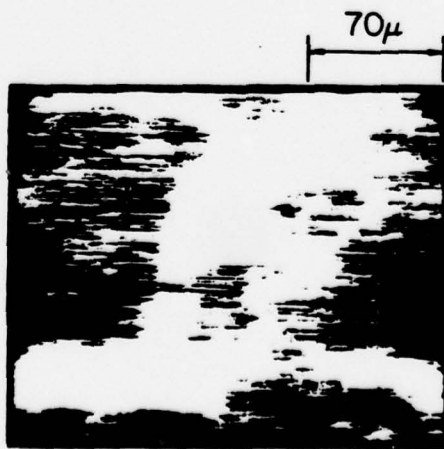
b) Fe-IMAGE 652 V



c) C-IMAGE 272 V



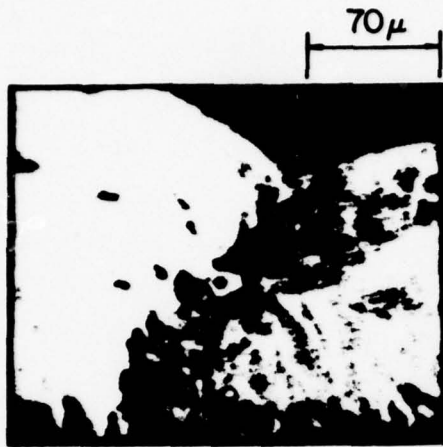
d) Ti-IMAGE 387 V



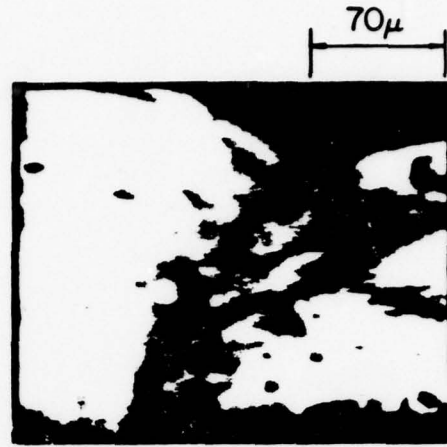
e) O-IMAGE 515 V

FIGURE 3

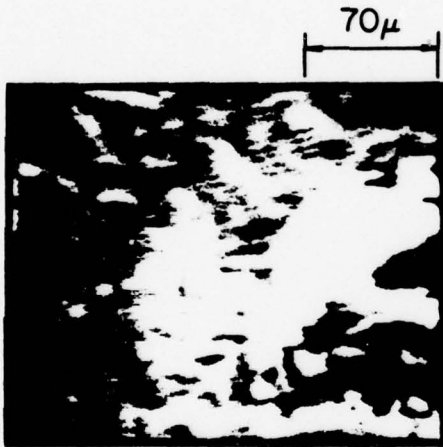
SEM/SAM ANALYSIS: PEBBLED SURFACE-NORMAL INCIDENCE ASPECT



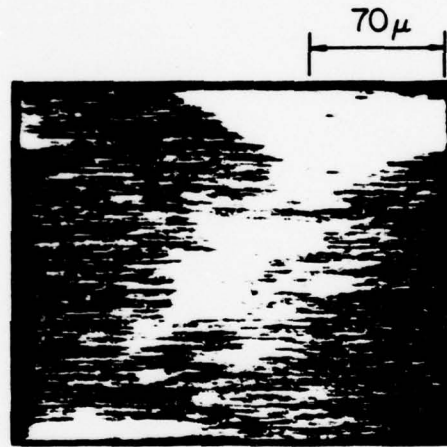
a) SEM TRACE - POINT C



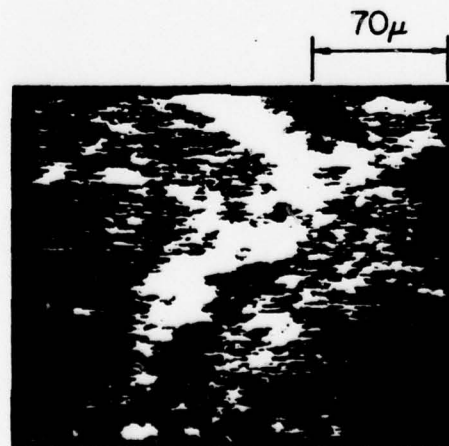
b) Fe-IMAGE 652 V



c) C-IMAGE 252 V



d) Ti-IMAGE 387 V



e) O-IMAGE 514 V

FIGURE 4

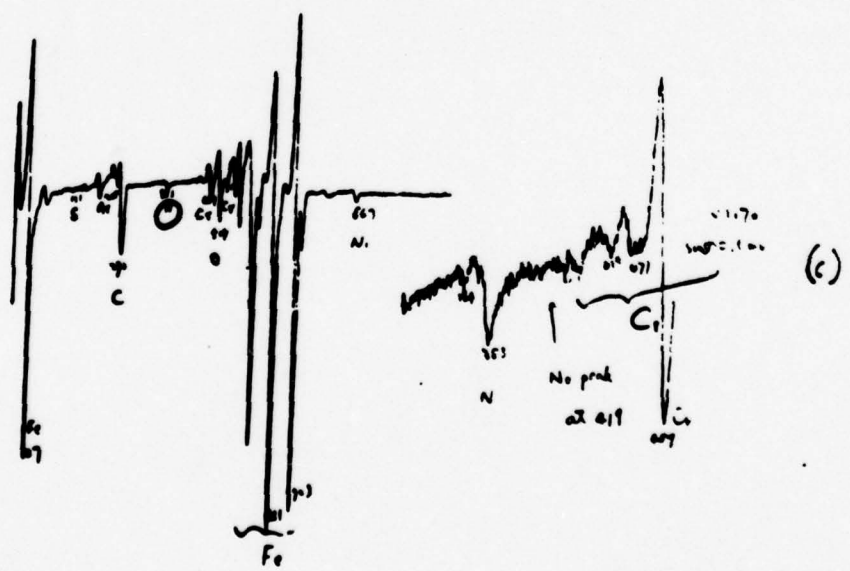
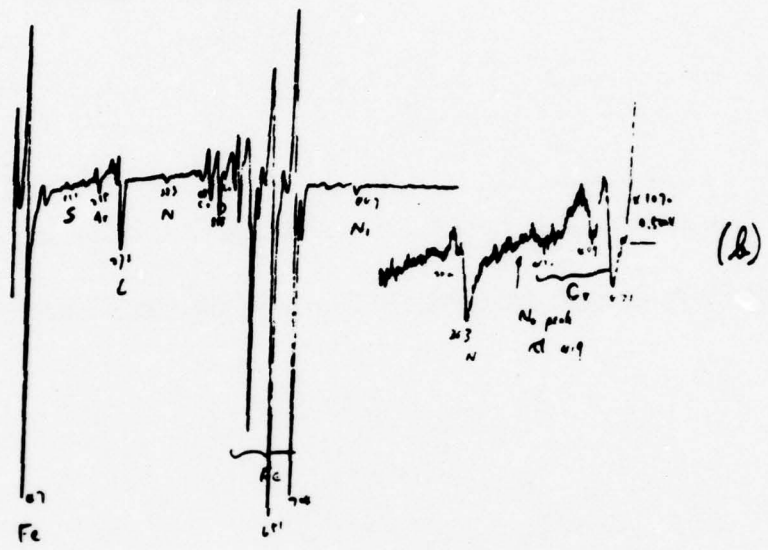
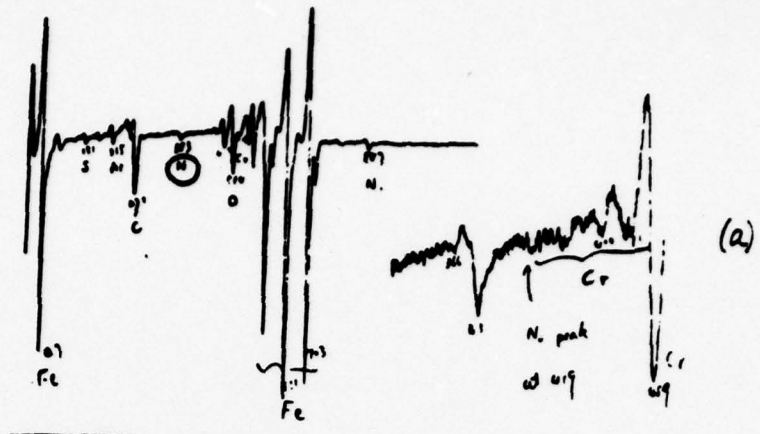
Panel b of Fig. 6 is an SEM image of crack A at higher magnification. The remaining photographs are N-(c), Fe-(d), C-(e) and O-(f) SAM images of crack A. The photographs of Figs. 7 and 8 are similar analyses of cracks B and C, both arranged as follows. Panels a are SEM images. The remaining photographs are N-(panels b), Fe-(panels c), C-(panels d) and O-(panels e) images.

Although there are clear differences in the elemental distributions in these cracks, there are also some common features. For example, the C-images all show that carbon is distributed along the entire length of each crack. The C-signals of AES traces of Fig. 5 are clearly carbide signatures indicating that the carbon in the cracks are most likely metal carbides that have segregated there during the embrittlement of the steel. On the other hand, the N-images all show nitrogen distributions that tend to aggregate at the middle of each crack. The nitrogen is probably in the form of metal nitrides which were formed by reactions between the metal on the crack surfaces and the nitrogenous constituents of the hot propellant gases under pressure during the firings. The absence of nitrogen at the open end of the cracks can be attributed to competing reactions with oxygen to form volatile components. This is suggested by the fact that the O-images show the oxygen more or less concentrated at the open ends of the cracks, in part bonded to carbon (because of the partial correlation with the C-images) and in part as iron oxides because of the correlation with the iron images. No Ti was detected in the cracks. At this point in our work it is not clear why. It may have to do with the fact that the cracks were not clearly correlated with the austenitic grain boundaries of the pebbled surface.

From these preliminary examinations of the surface cracks, it is evident that propellant reactant constituents are non-uniformly distributed in the cracks and that some of the chemistry occurring at the crack surfaces with the propellant gases can be traced by SAM techniques. Laying the crack surfaces bare by low-temperature fracture will yield additional information about crack formation and chemical activity at crack surfaces.

CROMIUM-COATED SURFACES

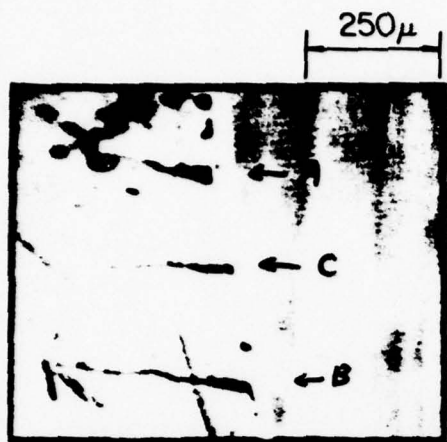
A section from a Cr-coated 105 mm M-68 barrel was also subjected to normal incidence SEM/SAM analysis. A low magnification SEM secondary emission image is shown in the photograph of Fig. 10, panel a. The AES trace from point B of the virgin surface is shown by trace a of Fig. 9. The AES trace of the sputter-cleaned surface is shown by trace b. Trace a shows the typical strong C- and O-signals of environmentally contaminated surfaces.



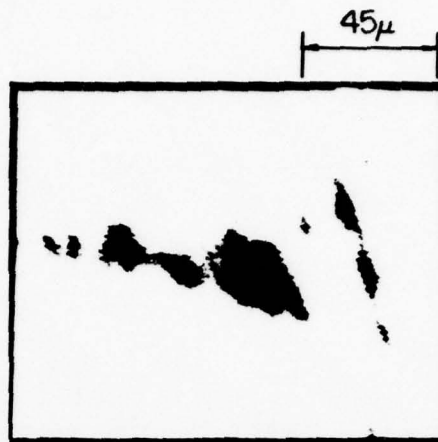
Pebbled Surface: AES traces from surface cracks
 sputter-cleaned surface
 (a)-point A (b)-point B (c)-point C

Figure 5

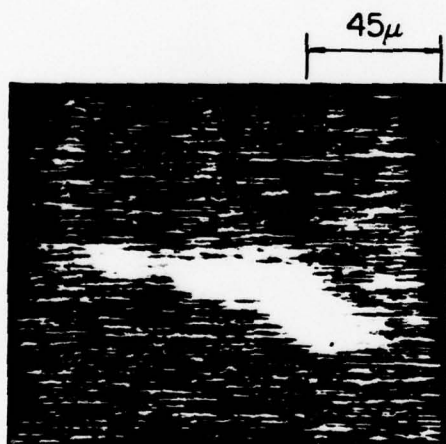
SEM/SAM ANALYSIS: PEBBLED SURFACE-TANGENTIAL INCIDENCE ASPECT



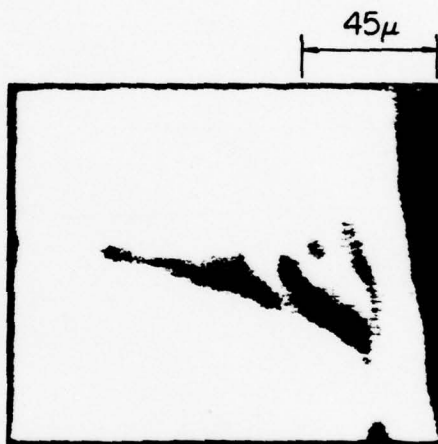
a) SEM IMAGE



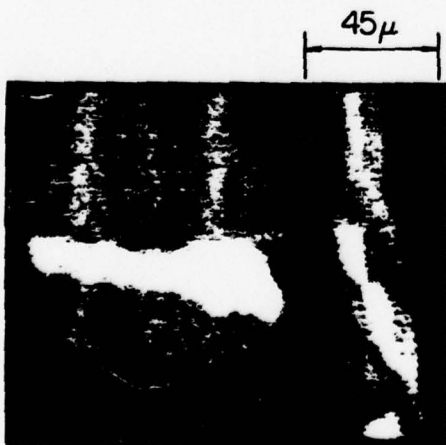
b) SEM IMAGE - CRACK A



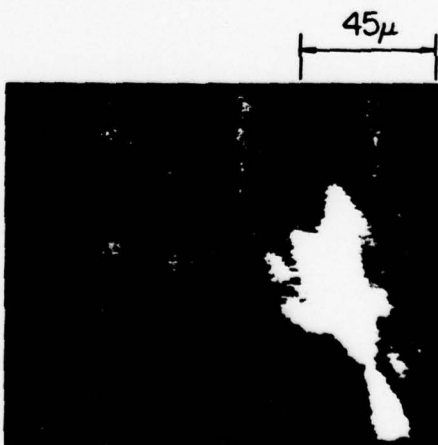
c) N-IMAGE 383 V



d) Fe-IMAGE 651 V



e) C-IMAGE 273 V



f) O-IMAGE 515 V

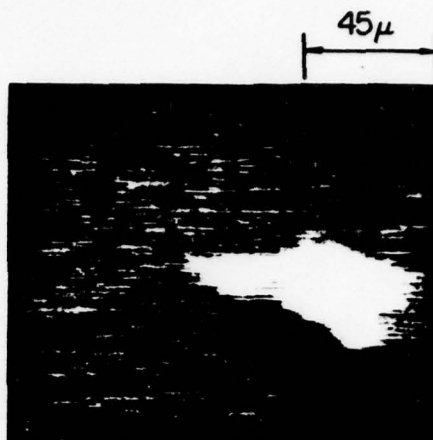
FIGURE 6

SEM/SAM ANALYSIS: PEBBLED SURFACE-TANGENTIAL INCIDENCE ASPECT

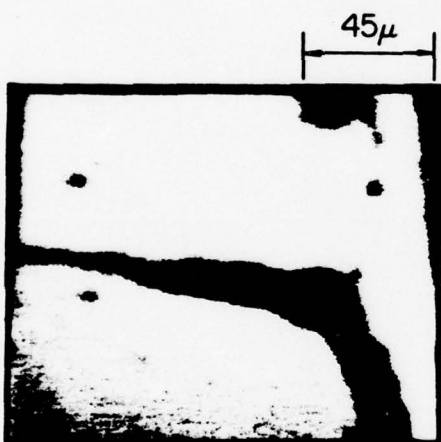
C



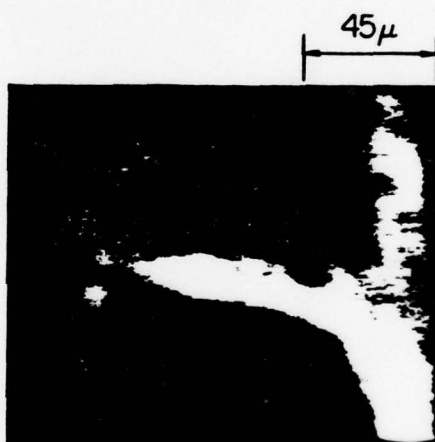
a) SEM IMAGE - CRACK B



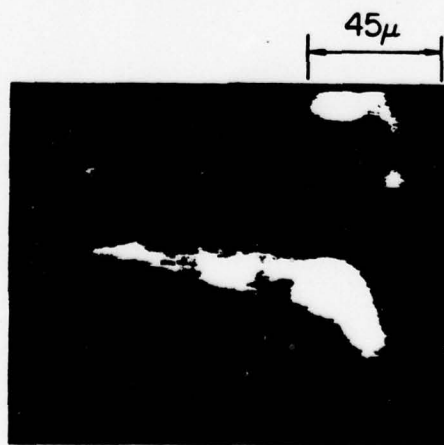
b) N-IMAGE 383 V



c) Fe-IMAGE 651 V



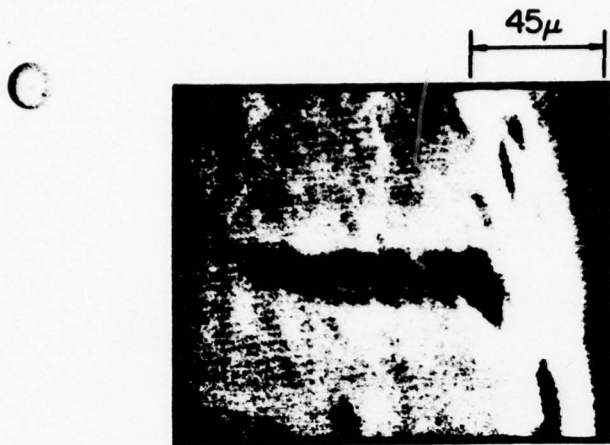
d) C-IMAGE 273 V



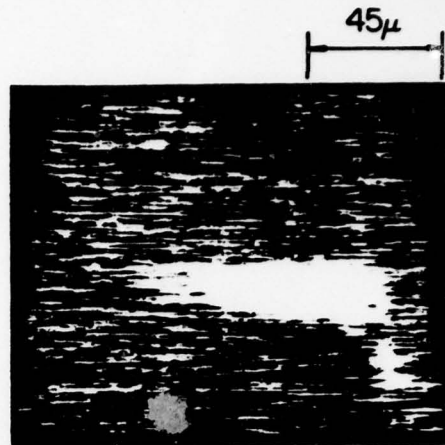
e) O-IMAGE 515 V

FIGURE 7

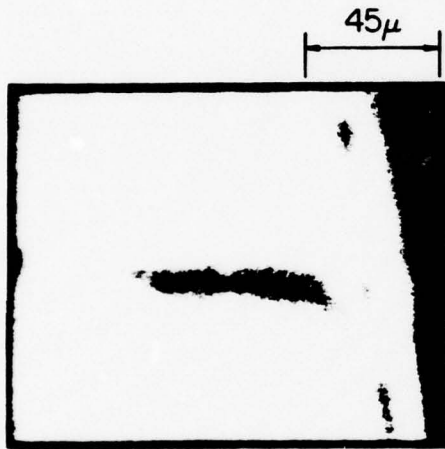
SEM/SAM ANALYSIS: PEBBLED SURFACE-TANGENTIAL INCIDENCE ASPECT



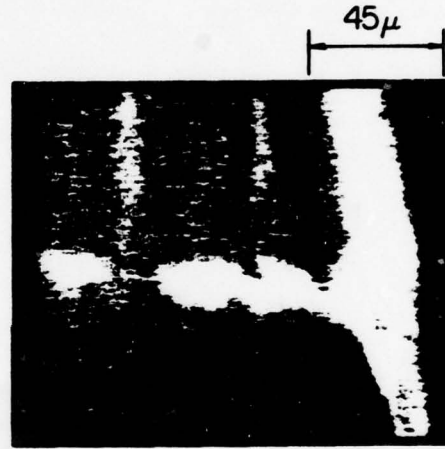
a) SEM IMAGE - CRACK C



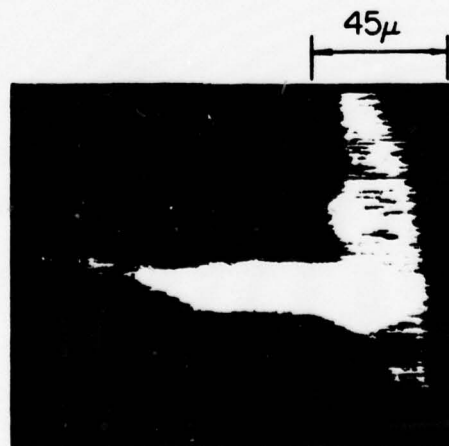
b) N-IMAGE 383 V



c) Fe-IMAGE 651 V



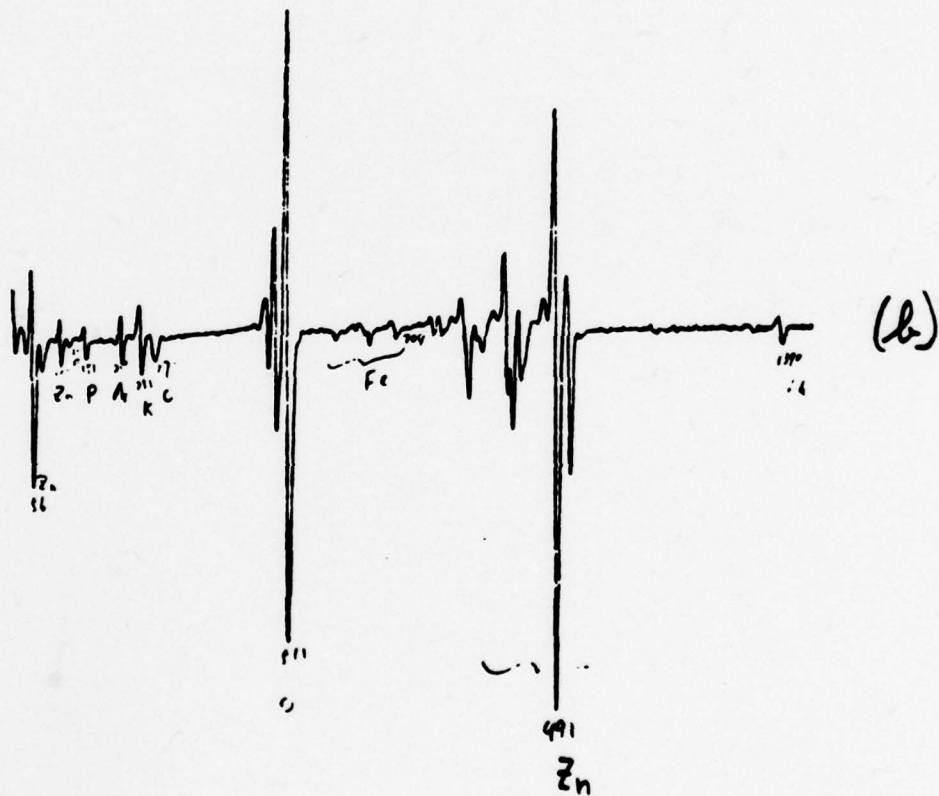
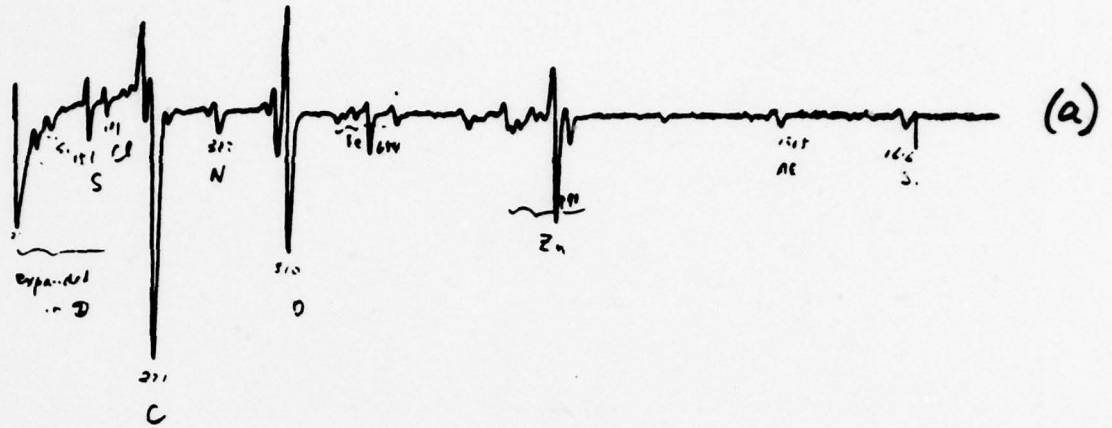
d) C-IMAGE 272 V



e) O-IMAGE 514 V

FIGURE 8

Cr-coated Surface: AES traces



(a) - virgin surface

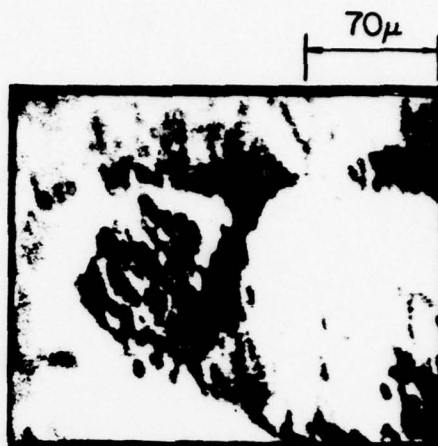
(b) - sputter-cleaned surface

Figure 9

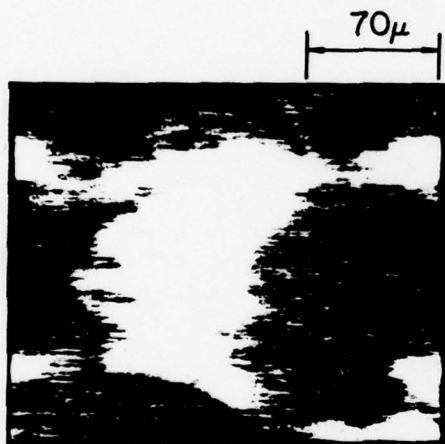
SEM/SAM ANALYSIS: Cr COATED SURFACE



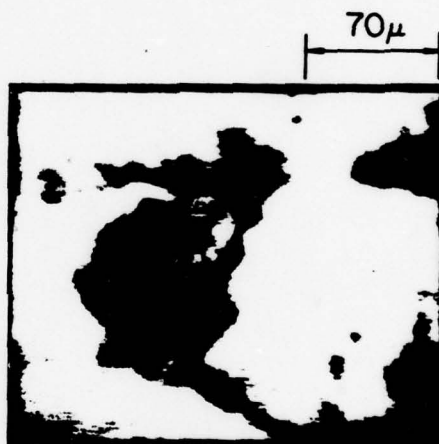
a) SEM IMAGE



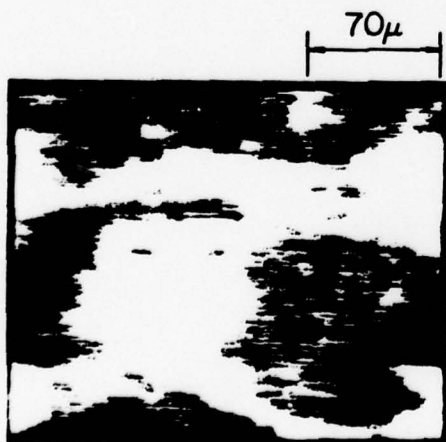
b) SEM IMAGE - POINT B



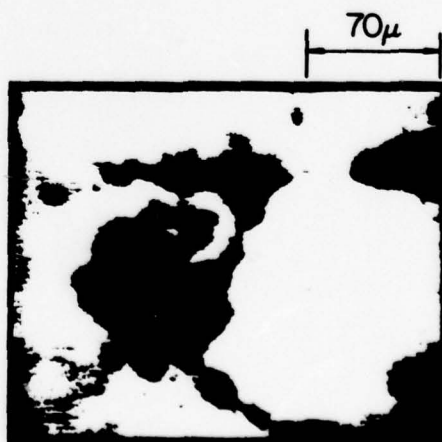
c) Fe-IMAGE 654 V



d) Zn-IMAGE 989 V



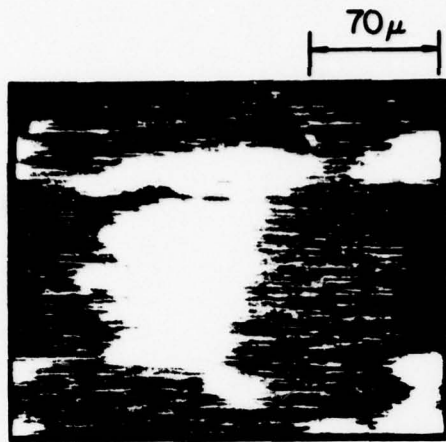
e) C-IMAGE 272 V



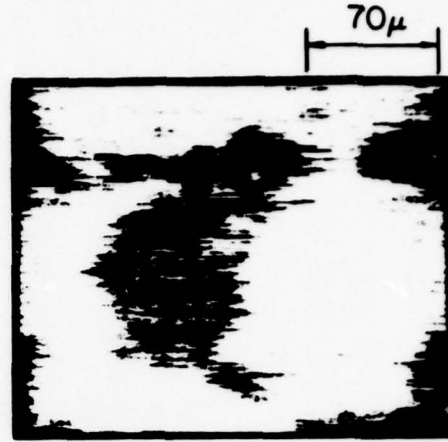
f) O-IMAGE 512 V

FIGURE 10

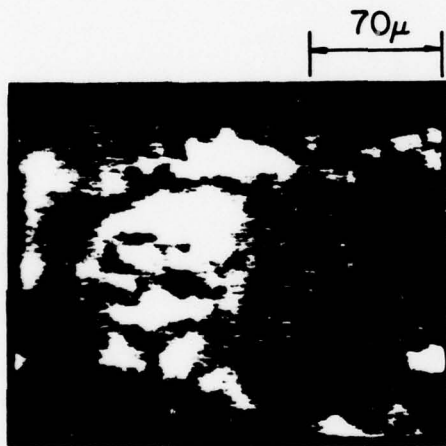
SEM/SAM ANALYSIS: Cr COATED SURFACE



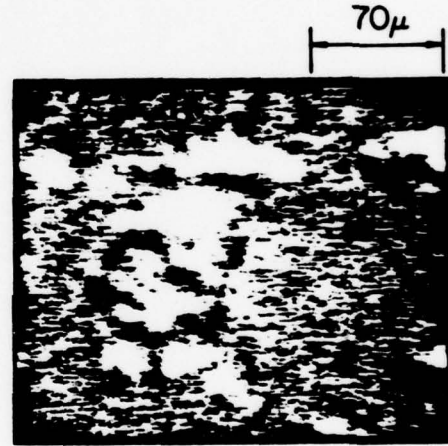
a) Ca IMAGE 292 V



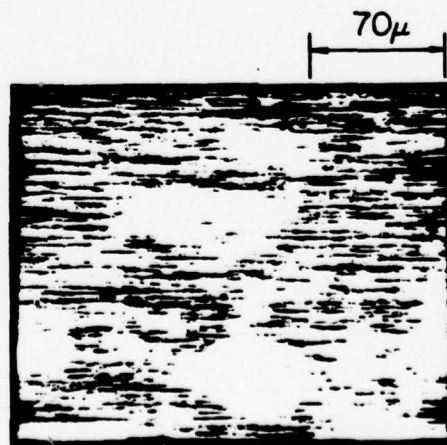
b) P-IMAGE 120 V



c) K-IMAGE 251 V



d) S-IMAGE 151 V



e) Al-IMAGE 1390 V

FIGURE II

Curiously, there is a Zn-signal (56V and the structure at 990V) that is stronger than the Fe-signal and no Cr-signal. Also, the low-voltage (56V) Zn-signal is very weak signifying a coated surface. The sputter-cleaned AES trace b shows an increased O-signal, indicating that at least some of the oxygen was not an environmental surface contaminant, and a decreased C-signal showing that the carbon was an environmental surface contaminant. That the surface has been cleaned of the environmental contaminant overlayer is shown by the increase in the 56V Zn-signal. The iron signal has not come up by sputter-cleaning and there is still no surface chromium evident on this nominally Cr-coated surface. Instead, the Zn- and O-signals have both come up clearly suggesting the presence of a tenacious ZnO coating.

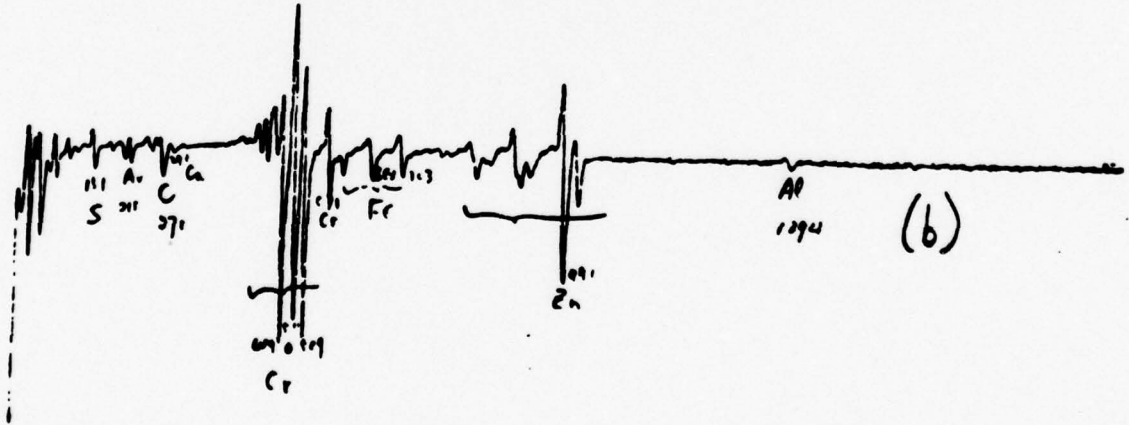
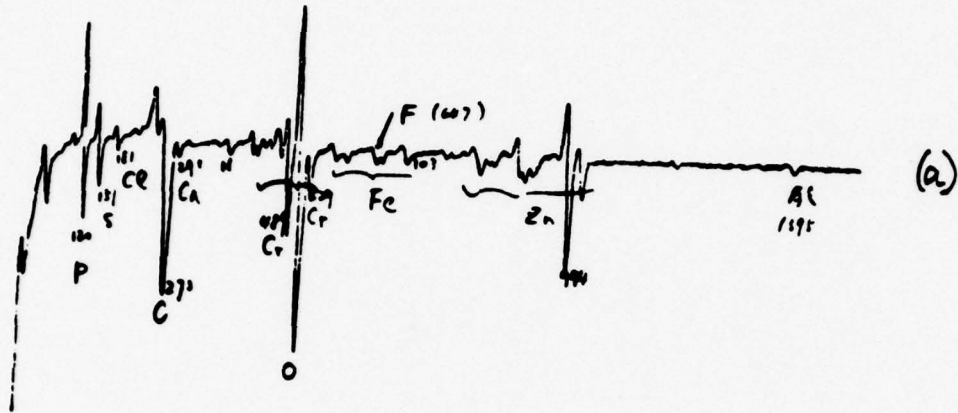
The existence of the ZnO coating is confirmed by the SAM-images of Fig. 10. Panel b of this figure is another SEM image of point B, panel a, at higher magnification. The remaining photographs show Fe-(c), Zn-(d), C-(e) and O-(f) images. These SAM images clearly demonstrate a correlation between the Zn- and O-images. Further, there is also a correlation between the Fe- and C-images. Additional SAM images of Ca-(a), P -(b), K-(c), S-(d) and Al-(e) are shown by the photographs of Fig. 11. These images show additional correlations among P, N and O, and among Fe, C, Ca, Al, K, and S. The ZnO coating most likely originates with the Zn-component of the brass cartridge casing, the Zn being oxidized during the combustion of the propellant.

The presence of the iron spec, the black areas of reduced secondary emission on the SEM images, suggest that the ZnO coating has either removed the Cr-coating and has laid bare the iron substrate. Alternatively, the Fe-patch could have come from the projectile which would allow the ZnO coating to be either on the Cr-coating or substituted for it.

To resolve these issues, the surface of the specimen was scratched with a diamond scribe. Panel a of Fig. 13 is an SEM image of the scratch. The surface damage is clearly evident. The virgin-surface AES trace is trace a of Fig. 12. It shows the strong C- and O-signals typical of environmental surface contamination. Also, a strong Cr-signal is now evident, suggesting that the original Cr-coating may have been revealed by the scratch.

These uncertainties are at least partially resolved by the remaining photographs of Fig. 13 which show the Zn-(b), Cr-(c), O-(d), C-(e), Fe-(f), S-(g) and Al-(h) images. The Zn- and O-images still correlate and show strong signals on either side of the scratch face. Concurrently, the Cr-image

Scratched Cr-coated Surface: AES traces

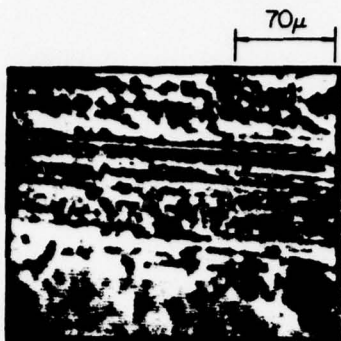


(a) - virgin surface

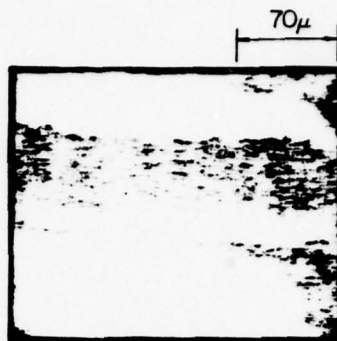
(b) - sputter-cleaned surface

Figure 12

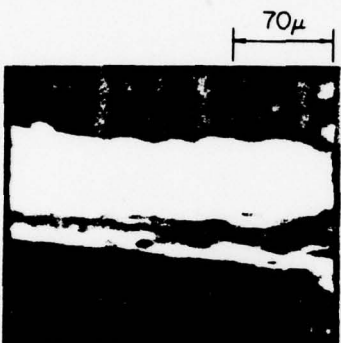
SEM/SAM ANALYSIS: SCRATCHED Cr-COATED SURFACE



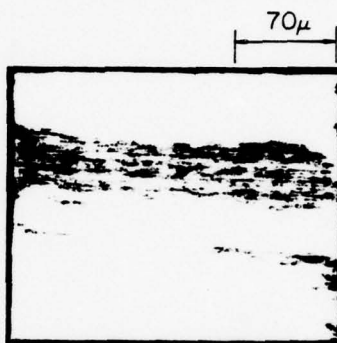
a) SEM IMAGE



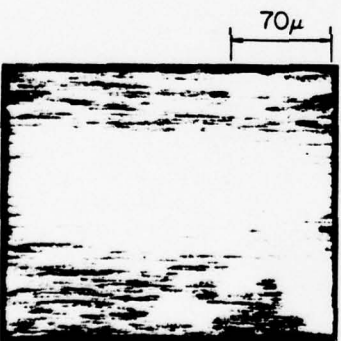
b) Zn-IMAGE 991 V



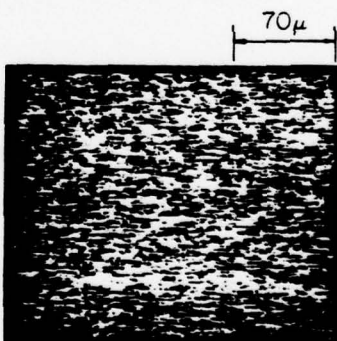
c) Cr-IMAGE 530 V



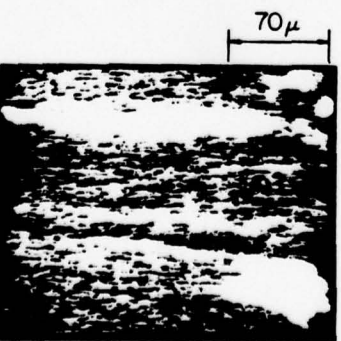
d) O-IMAGE 512 V



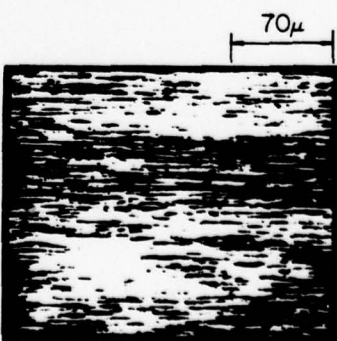
e) C-IMAGE 274 V



f) Fe-IMAGE 702 V



g) S-IMAGE 152 V



h) Al-IMAGE 1394 V

FIGURE 13

anticorrelates with the Zn- and O-images and shows a strong signal only from the scratch face. Thus, we may safely conclude that the ZnO coating, deposited during use, resides principally on the Cr-coating. It is not yet known what effect, if any, this tenacious ZnO deposit has on the wear-quality of the bore surface. To the author's knowledge, such ZnO deposits have not previously been observed by more conventional metallurgical diagnostics. It remains to be seen from further investigations whether the ZnO helps or harms the embrittlement problem and the flaking of the Cr-coating.

Some features of the remaining SAM images also should be noted. First, carbon appears to correlate with Cr, while Al appears to correlate with the ZnO. Sulfur appears in clumps, preferentially at the scratch boundaries. Finally, iron, which is clearly evident in the AES traces (Fig. 12) is very uniformly distributed over the surface as can be seen from the Fe-image, panel f, Fig. 13. (The reason the overall signal level appears low in the Fe-image is that signal contrast is needed over the surface to produce good image contrast). The reason for these characteristics are unclear at present and require further study.

SYNOPSIS

In this preliminary report, we have endeavored to demonstrate the usefulness of combined SEM/SAM analysis applied to bore surface wear and erosion examination. With bare bore surfaces exhibiting the pebbled texture of a worn bore, we have observed (apparently for the first time) the presence of the TiO_2 wear-reducing additive on the bore surface and have been able to specify that it resides in the austenitic grain boundaries of the embrittled steel. We have also demonstrated the ability of the SEM/SAM technique to profile the elemental distribution along cracks away from the bore surface.

With the Cr-coated specimen, which was sectioned from a barrel that has been fired with cartridge shells, we have observed (apparently also for the first time) a substantial and rather uniform ZnO coating on the original Cr-coating. The ZnO deposit presumably originates with the Zn-constituent of the brass cartridge casing. The effect of this ZnO deposit on the performance of the bore surface is not known at this time.

REFERENCES

1. Progress Report DAAG26-76-G-0017, 7/1/77-12/31/77.
2. C. J. McMahon and L. Marchut, J. Vac. Sci. Technol. 15, 450 (1978).

UNCLASSIFIED

Appendix C

SCANNING AUGER MICROSCOPY (SAM) STUDIES OF WORN BORE SURFACES*

P. Mark and J. L. Yeh
Department of Electrical Engineering
Princeton University
Princeton, New Jersey 08540

ABSTRACT

This paper reports the first results of the application of scanning Auger microscopy (SAM) to the study of wear and erosion of large caliber gun bore surfaces. Areal resolved elemental analyses of the worn bore surfaces reveal deposits of inorganic salts derived from various constituents of the propellant. In the case of fixed ammunition 105mm Cr-plated bore surfaces, the inorganic salt coating comprise a continuous film about 20 μm thick (~ 1 mil) consisting mainly of ZnO derived from the Zn plating of the propellant casing. Although the Cr plating is thinned during use, the inorganic salt coatings form on top of the Cr coating suggesting that they are wiped off and redeposited on each firing. Fracture studies reveal a metallurgically (thermally and/or mechanically) altered layer extending about 200 μm (~ 10 mil) below the bore surface at the breech end. This is about 10 times the thickness of the Cr plating remaining on the worn bore surface. The interface between the altered layer and the unaltered steel substrate cannot maintain a shear stress and resembles the interface between a brittle and a ductile phase. A similar fracture profile was observed with the specimen sectioned from the bore of a worn, uncoated 5-inch naval gun fired with bag charges containing a TiO_2 wear-reducing additive, thereby showing that the Cr coating does not influence the ultimate creation of a mechanically weakened interface in the gun steel parallel to the bore surface.

*) Supported by Army Research Office (Grant #DAAG29-79-G-0038)
Approved for Public Release.
Distribution Unlimited.

UNCLASSIFIED

UNCLASSIFIED

INTRODUCTION

Several analytical techniques have been applied to the study of wear and erosion of gun bore surfaces. The oldest and most widely used are conventional metallographic techniques which have established the existence of so-called altered layers at the surface whose mechanical hardness and microstructural properties differ from those of the virgin gun steel.¹ The altered layers are generally softer than the unaltered steel, possess a different metallurgical grain structure, and are characterized by microscopic and macroscopic cracks. These altered layers tend to extend about 200 μm (~ 10 mil) into the bore surface. When spalling is observed, the fracture generally occurs along the interface between the altered layer and the unaltered steel substrate. Although conventional metallographic analyses have revealed much useful information when applied to both field-tested specimens as well as in simulation studies, the origin of the altered layers has yet to be clarified. Specifically, it has yet to be established whether the altered layers are primarily of thermal origin² or of mechanical origin.³ One principal weakness of conventional metallographic studies is that little or no compositional information is derived from them.

Other, more modern techniques have been applied more recently to the study of wear and erosion. These include ESCA,⁴ nuclear activation analysis⁵ and Rutherford scattering.⁶ ESCA is an x-ray stimulated electron spectroscopy capable of obtaining an elemental analysis and of deriving chemical bonding information. It has been applied so far only in simulation studies comprising the exposure of various gun steels to burning propellants and the subsequent analysis of oxidation and corrosion reaction. The principal results have been to demonstrate that gun steel #4340 is more reactive than stainless steel #303 which, in turn, is more reactive than Allied Chemical MetGlass #2826A. It was also observed that the elements C, N and O are present as carbonyls, nitrides and oxides of the metals in the specimens. Most significant, perhaps, is the observation that chemical reactions continue to be observed as long as days after the initial exposure. Nuclear activation analysis exploits nucleon-induced transmutation to convert non-radioactive material constituents into radioactive isotopes for subsequent analysis. This technique has been applied to the study of wear rates. The virgin bore surface is exposed to 5.45 MeV protons which transform ^{56}Fe into radioactive ^{56}Co . As the proton range is short, transmutation occurs only in a superficial layer. As the tube is used, wear rates can be established by recording the decrease in ^{56}Co with use. The advantage of this technique is its simplicity; it is compatible with field testing conditions. It has been applied to small bore systems. Rutherford scattering analysis is an elastic ion scattering technique in which light ions (usually He^+) of several MeV energy are scattered from the specimen. The large-angle elastic scattering events are detected and, for a given scattering geometry in the laboratory coordinate system, the energy loss observed for the scattered ions is directly related to the atomic mass of the scattering species. Thus, Rutherford scattering is a simple (although expensive), non-destructive elemental analysis technique. It has found wide application in various thin film analysis problems particular to the

UNCLASSIFIED

UNCLASSIFIED

microelectronics industry. Recently, it has been used in simulation studies on the effects of propellant burn on the surface composition of gun steels.

In this paper we report the initial results of a program that applies scanning Auger microscopy (SAM)^{7,8} to the analysis of bore surfaces. SAM is the utilization of Auger electron spectroscopy (AES) in the scanning mode. AES is an electron-induced electron spectroscopy in which core electrons are ionized by electron excitation in the form of a well-collimated primary electron beam of several keV energy. The electron-induced core holes are neutralized by higher-lying core electrons or by valence electrons. The energy so released can be observed either as x-ray fluorescence or as internal conversion electrons, the so-called Auger electrons, which, like the characteristic fluorescence x-rays, emerge from the excited atom with characteristic energies. The Auger electrons can be energy analyzed to reveal an elemental analysis of the specimen. With sufficiently high resolution (and expensive) spectrometers chemical information can also be extracted from the Auger electron energies. As the Auger electrons generally have energies less than $\frac{1}{2}$ keV, their range in the specimen is limited to less than a few tens of Angstroms. Thus, the technique is very surface sensitive. Further, because the Auger electrons are electron-excited, by scanning the primary electrons and by imaging the Auger electrons synchronously with the primary beam on a kinescope, an areally resolved elemental image can be obtained. This is AES in the SAM mode. Finally, because one can collect all the secondary electrons as well as the Auger electrons in the same apparatus, one can compare the elemental images with the secondary electron images of the so-called scanning electron microscope (SEM) mode. Thus, elemental images and topographical images are capable of direct comparison.

This initial report presents preliminary results of the SEM/SAM technique applied to the analysis of a specimen sectioned from the breech end of the bore surface of a 105 mm tank gun that had been worn out by firing about 500 rounds with M-30 propellant. Subsequent to the surface analysis, the specimen was fractured and the fracture face was similarly analyzed and compared with the fracture face of a specimen sectioned from an uncoated, worn 5-inch naval bore. In the following sections, we describe the specimens, the firing conditions, the analytical apparatus, and the results of the surface and fracture analyses. The final section presents some conclusions that can be drawn from this work.

SPECIMENS

The Cr-coated specimen was sectioned 5 inches from the breech end of a worn 105 mm tank gun from which 500 rounds of fixed ammunition had been fired. The Cr-coating had been electroplated. Its original thickness was about 250 μm (~ 10 mil). M-30 propellant in a Zn-plated, steel casing was used. The rounds had plastic rotating bands. The specimen was sectioned from a rifling land and was about 3 mm wide, about 15 mm long and about 4 mm deep. The bore surface looked black to the eye, had a smooth, glossy finish and showed no evidence of spalling. The uncoated specimen was

UNCLASSIFIED

UNCLASSIFIED

sectioned from 5-inch naval gun that had been fired using a bag propellant that contained a TiO_2 wear reducing additive. It had roughly the same dimensions as the Cr-coated specimen. No further information about the naval specimen is known to the authors. The naval specimen surface looked shiny to the eye and had the characteristic pebbled texture of a worn surface (see panel a of Fig. 5). After surface analysis, both specimens were fractured in air using the fracture geometry illustrated by the top, left panel of Fig. 6. The fracture profiles were then analyzed by SEM to establish the strong similarity in the fracture properties of these specimens (see Fig. 7 and accompanying discussion).

ANALYTICAL APPARATUS

A Physical Electronics SAM was used in this work. The electron spectrometer was a single pass cylindrical mirror analyzer (CMA) with a coaxially mounted primary electron gun. The primary energy was 6 keV for all analyses and the primary beam diameter was 3 μm in the SAM mode. The specimens were mounted on a carousel stage for sequential analysis. The surfaces were sputter-cleaned with 1.5 keV argon ions in a background pressure of 5.0×10^{-5} torr ultra pure ("5-9's") argon that had been scrubbed by Ti-sublimation pumping. During analysis, the background pressure in the stainless steel, sorption-sputter-ion pumped vacuum station was in the high 10^{-10} torr range.

SURFACE ANALYSIS

Figure 1 comprises three AES traces obtained from the surface of the Cr-plated specimen under differing circumstances. Each trace represents a plot of (dN/dE) vs. E where N is the energy-dependent secondary emission distribution and E is the energy. This augmented first derivative curve is the direct output of the CMA. The characteristic structures observed in each trace can be attributed to given elements by comparison with published calibration spectra. Each of these structures is labelled with the appropriate element.

Trace a was obtained from the virgin surface, prior to sputter-cleaning. The trace shows several elements usually observed on any metallic surface that had been exposed to the atmosphere. These are C, O, N and Cl. Only a small amount of Fe and no Cr are present which may result from the presence of the surface contaminants. The large Zn signal cannot be attributed to atmospheric contamination.

Trace b was obtained subsequent to sputter-cleaning. It reveals several curious features. First, both the Zn and O signals are markedly increased. Thus the O signal of the virgin surface was not entirely from an atmospheric contaminant. Second, the C signal is much reduced indicating that the large C signal of the virgin trace did stem from atmospheric contamination. The C signal, when expanded to greater sensitivity (not shown), also had the distinctive chemical carbide signature. Third, the Fe signal has been reduced and traces of F have become evident. Fourth, other trace impurities have been revealed, namely, P, K, and Ca. The A impurity stems

UNCLASSIFIED

UNCLASSIFIED

from implanted sputtering ions. Also, the S and Cl signals of the virgin trace are gone indicating that these were atmospheric contaminants. The small Al signal of the virgin trace is still observed. Fifth, and perhaps most important, there is no evidence of Cr in trace b. This means either that the Cr-plating has been completely lost from the specimen surface through wear and erosion or that it is completely covered by a surface coating.

In order to get further insight into the nature of the surface coating, the sputter-cleaned specimen was subjected to SEM/SAM analysis. The results are shown in Figs. 2 and 3. Panel a of Fig. 2 shows an SEM image of the worn, Cr-plated surface. The image shows a dark structure on a white background. The dark structure is a flaw and it was decided to image the area near the flaw to provide image contrast. The white background of the SEM trace corresponds to the black optical appearance of the surface. The SEM background is white only because it has a higher secondary electron emission yield than the material comprising the flaw. Panel b is an SEM image under higher magnification of the region labelled "B" in panel a.

The remaining panels of Figs. 2 and 3 are SAM images of the various elements detected on the surface by the AES spectrum, trace b of Fig. 1. Each image is obtained by setting the CMA at the energy corresponding to the element in question and imaging the output signal of the CMA on the kinescope synchronously with the scanning primary beam. Panels d and f of Fig. 2 are the Zn and O images, respectively. The strong image intensity correlation of these two panels strongly suggests that the white background of the SEM images, which comprise by far the major portion of the specimen surface, is a layer of ZnO. More will be said about this ZnO coating in the section devoted to fracture analysis. In all likelihood, the ZnO coating stems from the Zn plating of the propellant casing which is oxidized during the combustion of the propellant and deposited on the bore surface as the reaction products cool. Panel b of Fig. 3 shows that the P image also correlates with the ZnO. However, as the P signal is much weaker than either the Zn or O signals, P is probably a contaminant and not a major constituent of a coating layer. The remaining panels of Figs. 2 and 3 display Fe, C, Ca, K, S and Al images which all correlate more or less with the dark flaw of the SEM image.

One may speculate on the origin of these elements. The Fe may be from the bore substrate in which case what has been called a flaw above may, in fact, actually be the bore surface from which the Cr plating has been removed. That this is not so will be demonstrated below. The C probably comes from the propellant, as do the remaining impurities. The F and Al come from the cryolite additive, the K from the black powder igniter, and the S from the black powder. The Fe is probably an iron spec that has flaked off from elsewhere in the breech area, probably from the casing, which has reacted with all the other elements that correlate spatially with it during the propellant combustion.

The principal unanswered question is: Why is there no Cr signal in the AES trace? Is it because the Cr has been worn away or is it because

UNCLASSIFIED

UNCLASSIFIED

the Cr is completely covered with other surface layers? To answer this question, the specimen was removed from the vacuum station and scratched with a diamond-tipped scribe. The specimen was then reinserted into the vacuum station, sputter-cleaned and reexamined with AES and SAM. Trace c of Fig. 1 is the AES trace obtained in the vicinity of the scratch. It clearly shows, first, the presence of Cr lines (near the oxygen signal), and second, a reduction in both the Zn and O signals. Further, all the impurities observed on the unscratched surface are also observed here.

The panels of Fig. 4 are SEM and SAM images of the specimen in the vicinity of the scratch. Panel a is an SEM image which clearly shows the topography of the scratch. Panels b and d are Zn and O images, respectively, which still correlate very well and which show that the diamond scribe has penetrated through the ZnO layer. Panel c is the Cr image which anti-correlates almost perfectly with the Zn and O images. Thus, we may conclude that the scribe has made a trench in the ZnO layer and has revealed the Cr plating underneath the ZnO layer; the ZnO comprises a coating over the Cr plating. The remaining images show, first, that the C image correlates well with the Cr image suggesting that there may be a chrome carbide layer on the Cr plating. In addition, the S trace appears to decorate the edges of the scratch suggesting that there is a sulfur-containing layer between the ZnO and the Cr. Finally, the Fe image is virtually uniform and the Al image, whose signal is near noise, appears here to correlate with the ZnO layer. More will be said on the composition of this apparently complicated coating in the discussion of the fracture analyses.

The specimen sectioned from the worn 5-inch naval gun was also subjected to SEM/SAM analysis. Panel a of Fig. 5 is an SEM image of the surface of this specimen and it clearly reveals the pebbled surface texture apparent on visual inspection. (This characteristic texture can also be seen in the lower panel of Fig. 7 which is an optical micrograph of the fracture profile of this specimen). The only unusual trace element observed in the AES spectrum of this surface (not shown) is Ti. Accordingly, an SAM analysis was performed of the region labelled "A" in panel a. Panel b is an enlarged SEM trace of the vicinity of point "A". Attention has been focused on the boundaries between the pebble domes.

Panel d of Fig. 5 is the Fe image. It clearly shows that the pebble domes are predominantly iron with impurity specs distributed over their surfaces. Trace c is the C image which reveals, first, that the impurity specs on the pebble domes are carbonaceous material, and second, that substantial amounts of carbonaceous materials are concentrated at the pebble boundaries. Panels e and f are Ti and O images, respectively. Their areal correlation is sufficiently good to suggest that these images represent TiO_2 and that it may be concluded that the TiO_2 wear reducing additive used in the propellant ultimately resides predominantly in the pebble boundaries. Note that there is no continuous coating on this specimen as there is on the Cr-coated specimen.

UNCLASSIFIED

UNCLASSIFIED

FRACTURE ANALYSIS

The fracture analyses were undertaken for two reasons. First, by creating a fracture face more or less perpendicular to the bore surface, it becomes possible to perform a compositional analysis of the Cr-plated specimen to determine the depths of the various layers observed over the Cr plating with the surface analysis. One can also assess the thickness of the residual Cr layer of the worn bore. The second reason is to obtain the fracture profile itself to determine what role, if any, the Cr plating plays in the metallurgy of the fracture mode. The role, or lack of it, played by the Cr plating was further investigated by also obtaining the fracture profile of the uncoated specimen and comparing this with the profile of the Cr-plated specimen.

The geometry is illustrated schematically by the top, left panel of Fig. 6. The specimens were fractured with the force components shown in this panel which resulted in a tensile force parallel to the bore surface. The fracture profile observed with both specimens is shown schematically by the top, right panel of Fig. 6. An enlargement in the vicinity of the bore surface is shown schematically by the bottom panel and will be discussed below after the experimental information has been presented. At this point what is important is that both specimens had similar fracture profiles as illustrated by the top, right and bottom panels of Fig. 6. There is an "altered layer" about 200 μm deep whose fracture face was nearly perpendicular to the surface tensile force. This can also be seen from the optical micrographs of Fig. 7, which show the fracture surfaces of the Cr-plated specimen and of the unplated specimen in the top and bottom panels, respectively. Below the altered layer, the fracture face is nearly parallel to the tensile force for both specimens. This indicates that the altered layer is brittle and that the interface between the altered layer and the unaltered substrate cannot sustain a shear force. This same interface is parted when material is spalled from the bore surface.

Another similarity in the fracture modes of these two specimens is apparent. The uncoated specimen (bottom panel, Fig. 7) reveals that the altered layer fractures along the pebble boundaries. A careful examination of the Cr-plated specimen (top panel, Fig. 7) clearly shows the existence of fracture areas near the fracture face that have the same dimensions as the pebbles of the uncoated specimen. Thus, it is likely that the Cr-plated surface also develops a pebbled texture but that it is less apparent because of the rather thick additional coating deposited on this surface during use, principally the ZnO layer. Thus, it appears that the presence of the Cr plating has little or no effect on the fracture mode although it does appear to extend the life of the bore surface until fracture (spalling) occurs.

To probe this conclusion further, a SAM analysis of the fracture face of the Cr-plated specimen was also performed. This is described best with reference to Fig. 8 which is a composite showing a reproduction of the optical micrograph (top panel, Fig. 7) in the lowest image, an SEM image obtained in a high-resolution, AMR scanning electron microscope viewed from

UNCLASSIFIED

UNCLASSIFIED

almost directly above the specimen surface, shown in the middle image, and an SEM image obtained in perspective in the SAM apparatus, shown in the top image. An AES trace obtained from the vicinity of the point labelled "G" on the upper SEM image is also shown on the composite. The AES trace shows the presence of Fe, Zn, O, Cr and C in addition to trace impurities. An AES trace taken in the vicinity of the point labelled "H" revealed only Fe. The point "H" is located at the sheared interface parallel to the bore surface between the altered layer and the unaltered steel substrate.

The SAM images were obtained in the vicinity of point "G". These are shown in Fig. 9. Panel a of this figure is a reproduction of the SEM image shown as the top panel of Fig. 8. Panels b and c are SEM images of point "G" at progressively higher magnifications. In panel c, we are looking at the top edge of the fracture profile where the flat, top bore surface meets the fracture face of the altered layer almost at right angles. A close examination of this SEM image reveals an elevated ledge at the left of the image, defined by a vertical face approximately $10\ \mu\text{m}$ ($\sim 0.5\ \text{mil}$) high. At the foot of that ledge is a second ledge that runs forward to the fracture surface of the altered layer. Panels d and f are SAM images of Zn and O, respectively. These correlate well with each other, and also with the raised ledge at the left of the SEM image of panel c. Thus, the very top surface layer near the fracture face is the ZnO layer and these images suggest that it is about $10\ \mu\text{m}$ ($\sim 0.5\ \text{mil}$) thick. Panel h is the SAM image of Cr. It correlates very well with the ledge observed in the SEM image (panel c) to the right and below the ZnO ledge. Further, the thickness of the Cr layer can also be estimated at about $10\ \mu\text{m}$ ($\sim 0.5\ \text{mil}$). Thus, we see that a piece of the brittle ZnO layer has flaked off at the edge during the fracture process revealing the Cr layer underneath. This flaking is also evident from the SEM image shown in the middle panel of Fig. 8. We may now associate the smooth texture, darker portions of the top surface of this image with the ZnO layer, and the lighter, more matte textured portions with Cr layers from which the ZnO layer has been flaked away by the fracture process.

Panels e and g of Fig. 9 are SAM images of C and Fe, respectively. They are seen to anticorrelate almost exactly and arise entirely from the vertical fracture face of the altered layer. The anticorrelation of the C and Fe images is an artifact of the experiment. As already mentioned, the fracture itself was performed in air so that the fracture face was exposed to atmospheric contamination. After reinsertion into the vacuum station, the specimens were again sputter-cleaned to remove this contamination. The direction of incidence of the argon ion sputter beam relative to the images of Fig. 9 was from above and to the right. Thus, the top surface was sputtered clean, as can be seen from the fact that it is carbon-free, but the fracture face was sputtered clean only where it slopes away to the right as viewed by the reader. The regions sloping away to the left were in the shadow in this geometry and hence retained the carbon contamination. This is clearly evident from an intercomparison of panels c, e and g. Thus, we conclude from this SEM/SAM analysis of the fracture face that most of the fracture face of the altered layer is iron (steel) and that the sheared surface (point "H", panel a) exposed by the fracture process is well below the Cr-steel interface.

UNCLASSIFIED

UNCLASSIFIED

This conclusion is summarized by the bottom panel of Fig. 6, which is a schematic drawing of the specimen along a fracture profile. The top layer is a rather brittle ZnO coating. Underneath that is usually, but not always, a second coating comprising sulfur-containing material. Its composition is not known. This sulfur-containing layer is not evident in the analysis embodied in the SAM traces of Fig. 9. However, it has been observed on other portions of the specimen surface from which the ZnO coating had been flaked off or scratched away (panel g, Fig. 4). This is followed by the Cr coating. These three layers are approximately equally thick. However, as the figure shows, the total thickness of the three layers accounts for only about 10% of the entire altered layer which extends about 250 μm (~ 10 mil) into the bore surface. Note also that the thickness of the Cr coating has been significantly reduced from its original value of 250 μm (10 mil). This probably means that the ZnO and sulfur-containing layer is wiped off during each firing, together with a portion of the Cr plating, and that the ZnO and sulfur-containing layer then recondense onto the bore surface after each firing.

SUMMARY AND CONCLUSIONS

We have used SEM/SAM analyses to demonstrate that:

(1) The surface of a fixed ammunition, 105 mm Cr-plated bore surface is covered with a layer of inorganic salts on top of the Cr coating comprising ZnO and possibly the phosphides of calcium and potassium, and also sulfur-containing compounds. These coatings are apparently reaction products of various constituents of the propellant charge and other components in the breech at the time of combustion. The coatings are apparently deposited on the bore surface as these combustion products cool, and as the breech pressure drops during the passage of the shell out the gun tube. The effects of these coatings on barrel life are unknown at this time.

(2) Inorganic deposits have also been detected on the surface of an uncoated, 5-inch naval gun which had been fired with bag charges containing a TiO_2 wear reducing additive. Specifically, the worn surface shows the characteristic pebbled texture and traces of TiO_2 were identified as residing in the boundaries between the pebble domes. However, no continuous coatings were observed.

(3) Fracture studies with the 105 mm Cr-coated specimen reveal that a pebbled surface texture may well also exist below the ZnO surface coating. The same fracture studies reveal that the altered layers extends to depth into the bore surface roughly 10 times that of the residual Cr coating after about 500 rounds have been fired, and at the same time that the Cr coating has been reduced to about one-tenth of its original thickness.

(4) Comparative fracture studies of the Cr-coated specimen and of the uncoated specimen reveal that essentially the same metallurgical changes have occurred. The altered layer in both cases is comparably thick. The altered layers separate along pebble grain boundaries which cannot sustain

UNCLASSIFIED

UNCLASSIFIED

a tensile force. The interface between the altered layer and the unaltered substrate is a steel-steel interface that cannot sustain a shear force and thus has the properties of an interface between a brittle phase and a ductile phase. This interface is parted when material is spalled from the bore surface.

(5) There is no evidence that the Cr-steel interface is in any way mechanically weakened. No evidence for flaking of the chromium at the Cr-steel interface has been observed.

(6) There is also no evidence whether the altered layer is of thermal or mechanical origin.

On the basis of these results one may speculate on the role of the Cr-coating in prolonging barrel life. If the altered layer is of thermal origin, it probably originates from the thermal cycling the bore surface undergoes at each firing. Very probably, the melting point of the gun steel is exceeded during each firing for a few milliseconds to a depth of about 200 μm (~ 10 mil), long enough to produce the phase change but not long enough to allow the full development of the shear strain in the altered layer. The Cr-coating apparently does not melt and so serves as a more or less solid skin over the altered layer. In the initial stages of bore life, the isotherm corresponding to the melting point of the gun steel lies entirely in the Cr coating. With increasing use, the Cr coating is thinned and the melting point isotherm moves inward through the Cr-steel interface into the steel substrate. At this point, the altered layer begins to form. With continuing use, the melting point isotherm continues to move into the substrate as the Cr continues to thin and the altered layer thickens accordingly. At this point, the major role of the Cr coating appears to be that of a solid skin over a momentarily melted substrate the principal action of which is to prevent the full effects of the mechanical shear force of the passing shell to act on the altered layer. On further use, areas develop on the bore surface where the Cr coating has been completely worn away. Here the bore surface is no longer protected by a solid skin and the full effect of the shear force of the passing shell can develop across the altered layer. The ultimate failure is then spalling, that is, the gross removal of material from the bore surface revealing a fracture plane parallel to the bore surface coinciding with the interface between the altered layer and the unaltered gun steel substrate.

ACKNOWLEDGEMENTS

The authors would like to thank Dr. I. Ahmed for supplying the specimens, and Drs. Ahmed, J. Sharma, J. Lannon, R. S. Montgomery and A. Niiler for useful discussions.

REFERENCES

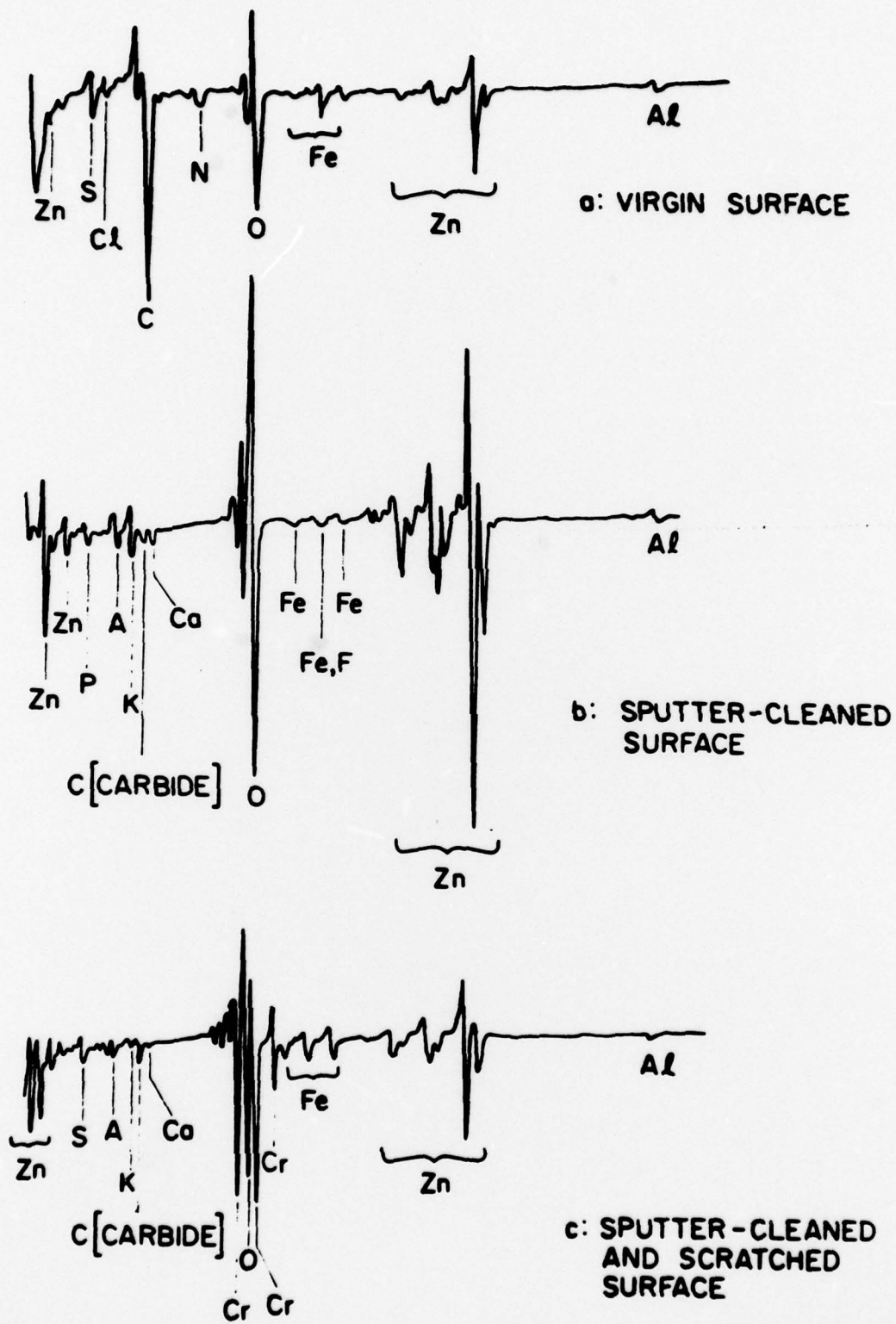
1. See the relevant papers in: PROCEEDINGS OF THE TRI-SERVICE GUN TUBE WEAR AND EROSION SYMPOSIUM (U.S. Armament Research and Development Command, Dover, NJ, 1977), J-P Picard and I. Ahmed, eds.

UNCLASSIFIED

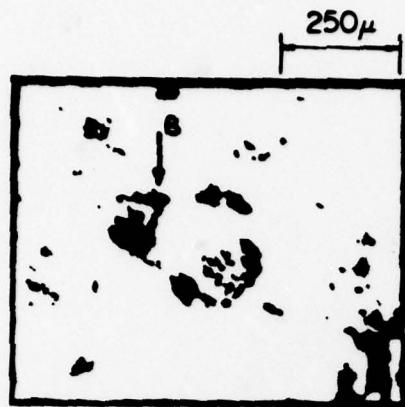
UNCLASSIFIED

2. See paper by I. Ahmed in ref. 1.
3. R. S. Montgomery and F. K. Sautter, to be published in Wear.
4. See paper by J. Sharma in ref. 1.
5. See paper by R. Birkmire and A. Niiler in ref. 1.
6. See paper by A. Niiler and R. Birkmire in ref. 1.
7. D. F. Stein, J. Vac. Sci. Technol. 12, 268 (1975).
8. C. J. McMahon and L. Marchut, J. Vac. Sci. Technol. 15, 450 (1978).

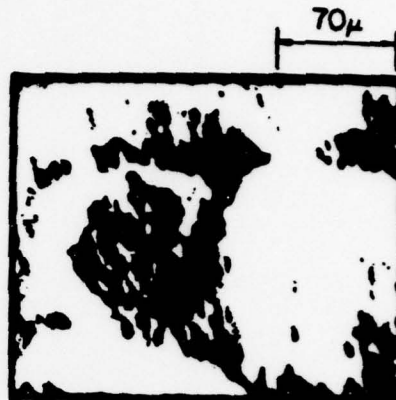
UNCLASSIFIED



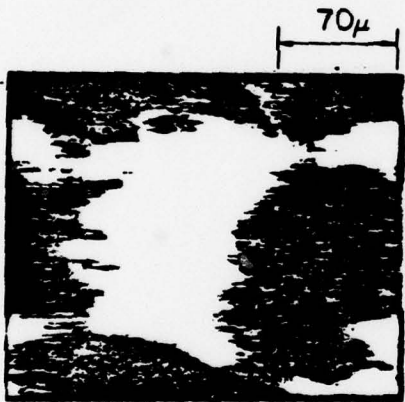
1. AES traces of Cr-plated 105 mm bore surface.



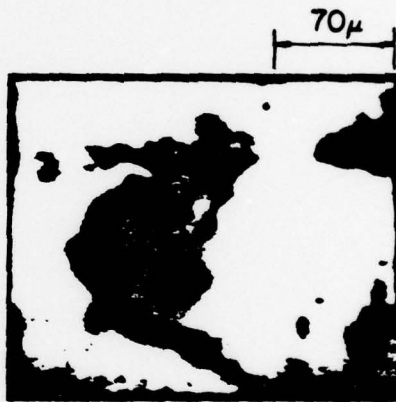
a) SEM IMAGE



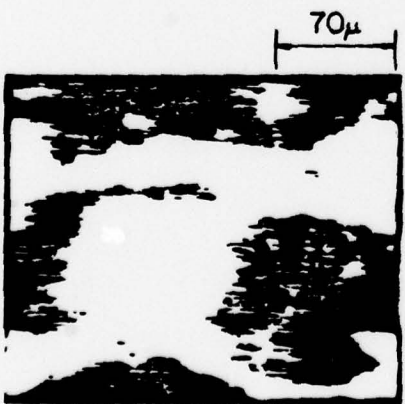
b) SEM IMAGE - POINT B



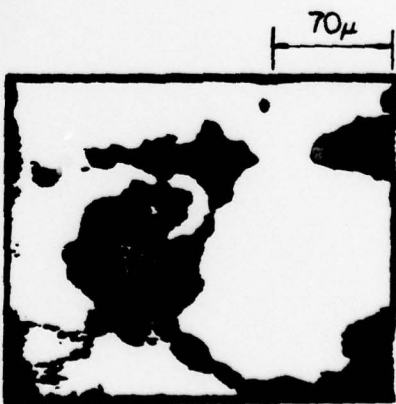
c) Fe-IMAGE 654 V



d) Zn-IMAGE 989 V

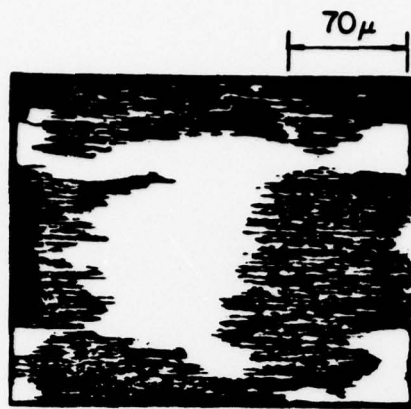


e) C-IMAGE 272 V

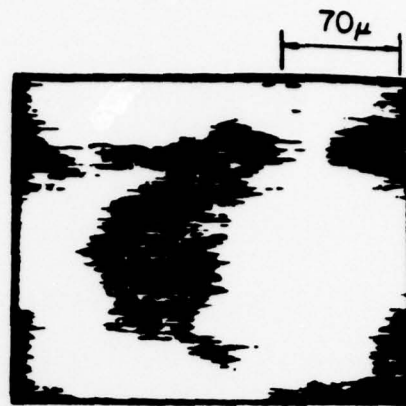


f) O-IMAGE 512 V

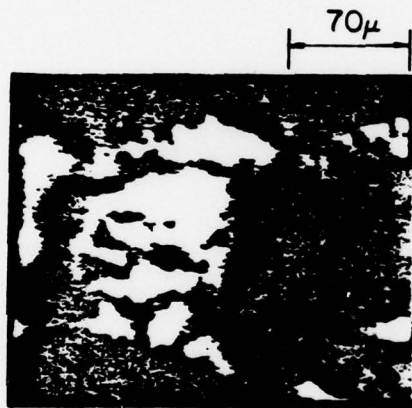
2. SEM/SAM analysis of Cr-plated 105 mm bore surface.



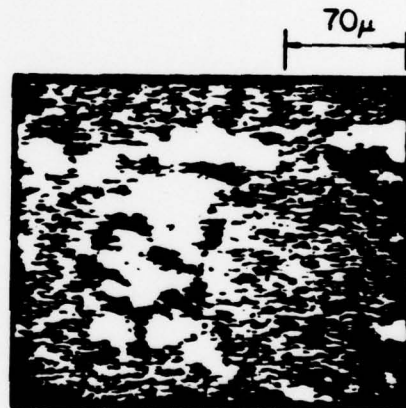
a) Co IMAGE 292 V



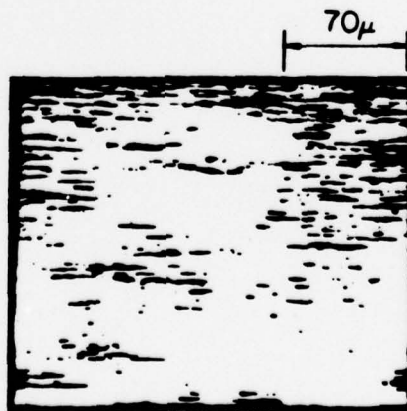
b) P- IMAGE 120 V



c) K- IMAGE 251 V

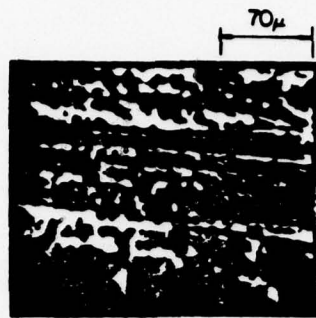


d) S- IMAGE 151 V

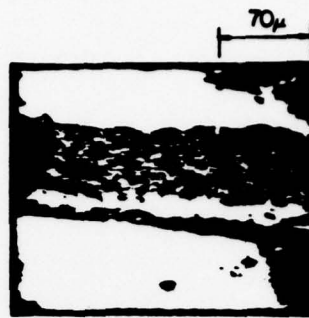


e) Al- IMAGE 1390 V

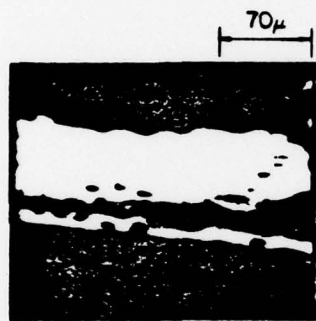
3. SAM analysis of Cr-plated 105 mm bore surface.



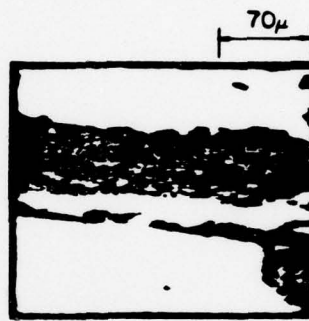
a) SEM IMAGE



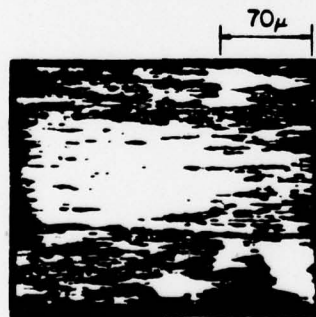
b) Zn-IMAGE 991 V



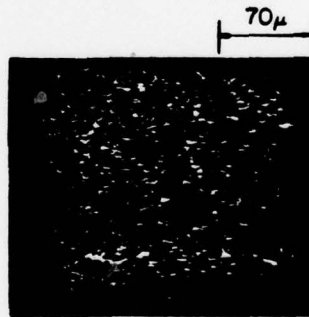
c) Cr-IMAGE 530 V



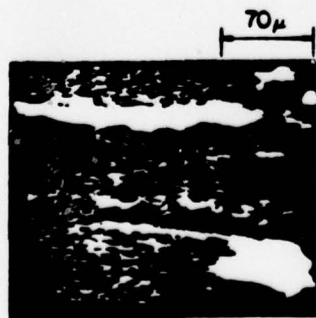
d) O-IMAGE 512 V



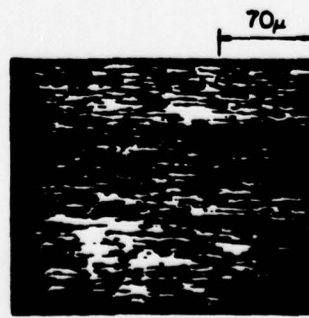
e) C-IMAGE 274 V



f) Fe-IMAGE 702 V

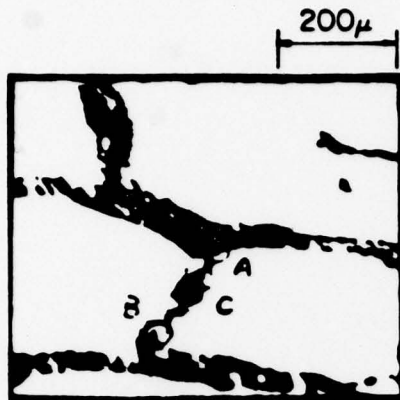


g) S-IMAGE 152 V

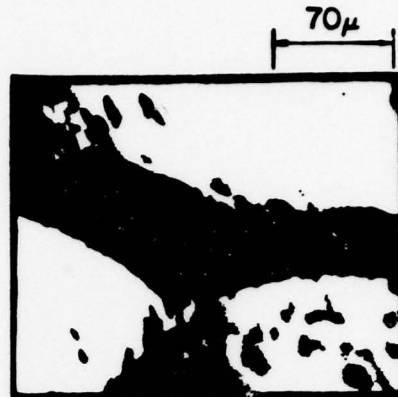


h) Al-IMAGE 1394 V

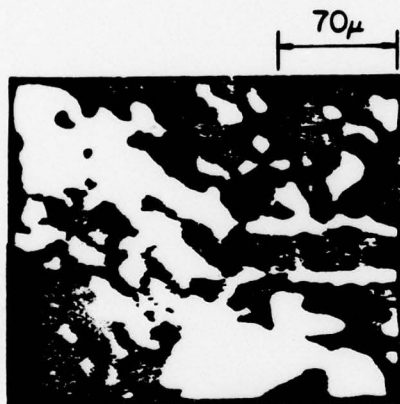
4. SEM/SAM analysis of scratch on Cr-plated 105 mm bore surface.



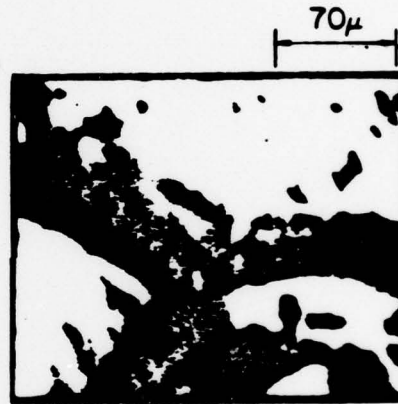
a) SEM IMAGE



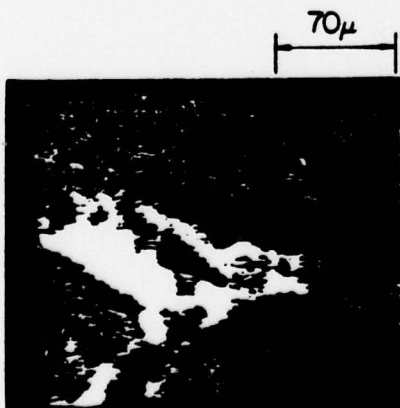
b) SEM IMAGE - POINT A



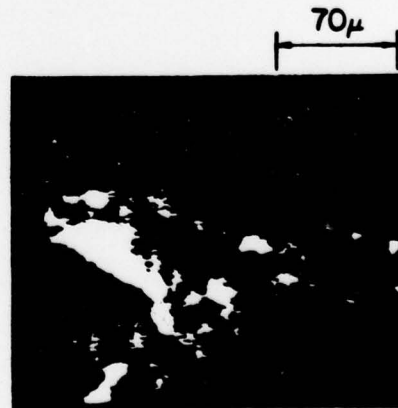
c) C-IMAGE 272 V



d) Fe-IMAGE 652 V

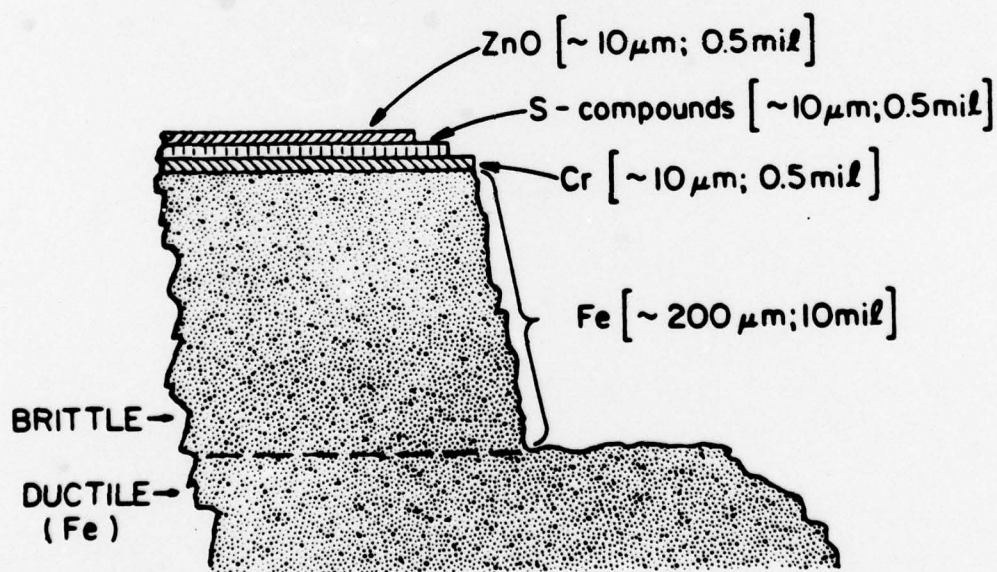
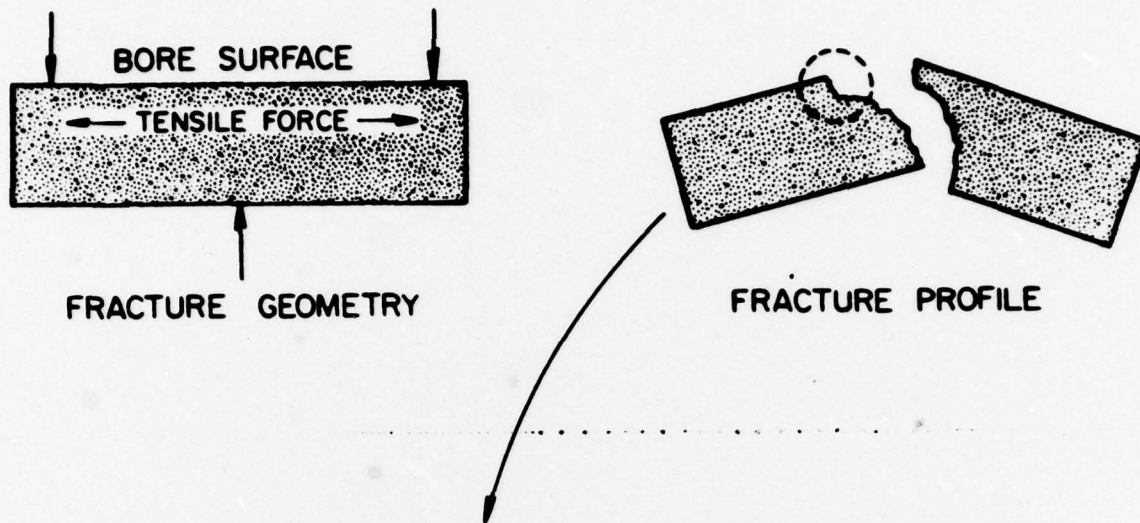


e) Ti- IMAGE 387 V



f) O-IMAGE 514 V

5. SEM/SAM analysis of uncoated, 5-inch naval gun bore surface.

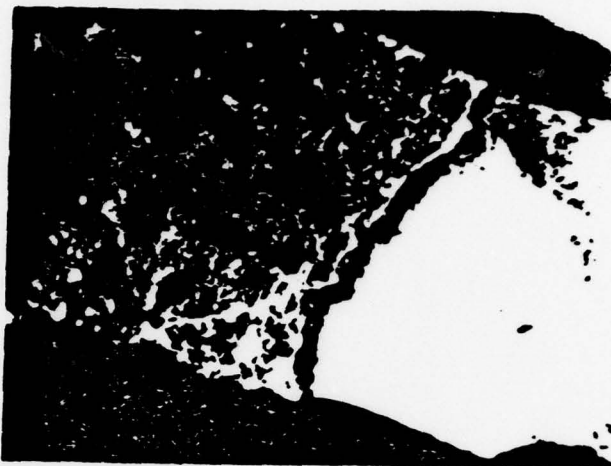


FRACTURE ANALYSIS

6. Schematic sketches of fracture analysis.

Cr-PLATED 105 mm

1 mm OPTICAL



5" NAVAL

OPTICAL 1 mm



7. Optical micrographs of fracture profile. Top panel: Cr-plated 105 mm bore surface. Bottom panel: uncoated bore surface.



Top image: SEM image recorded in SAM system.

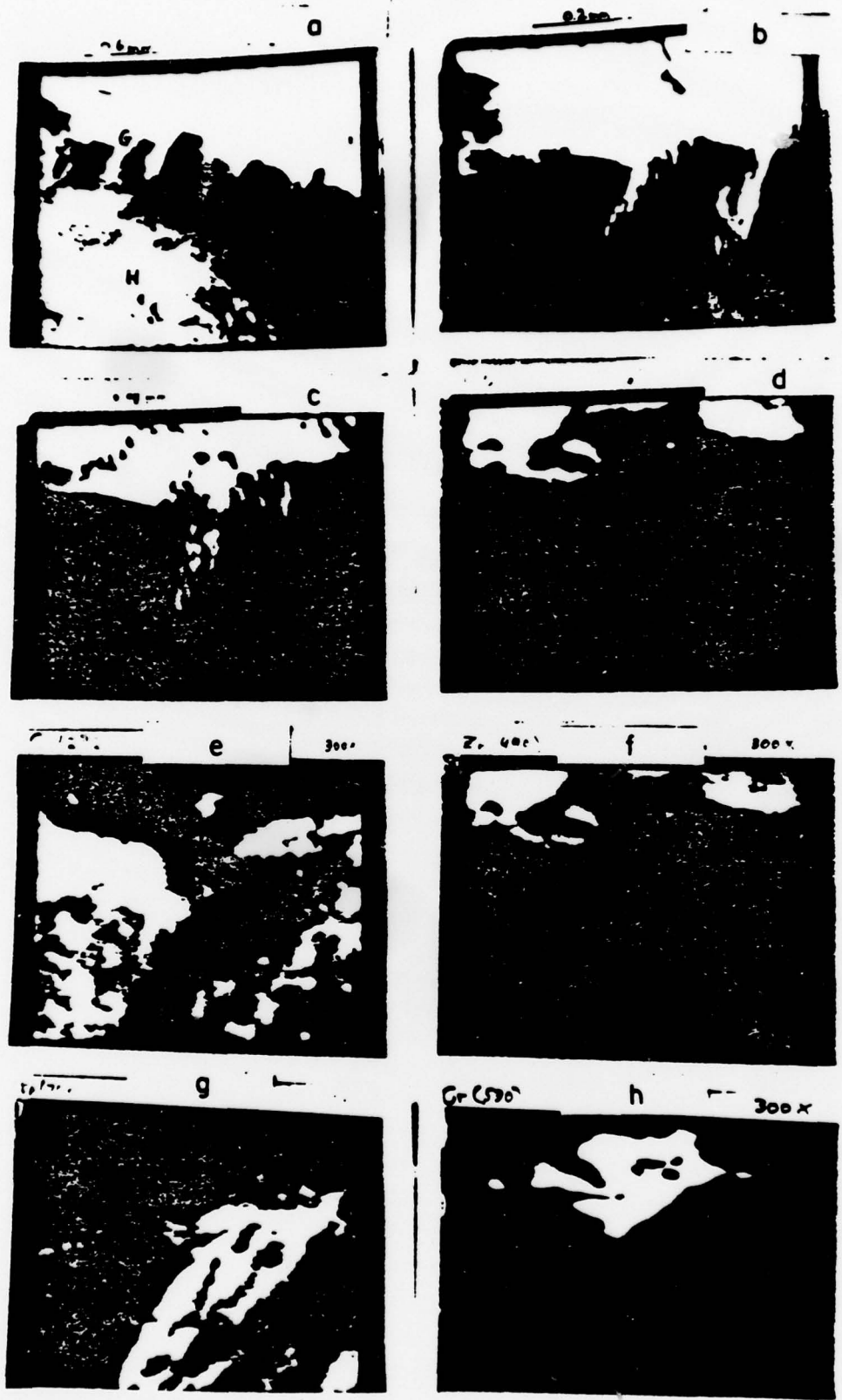
Middle image: SEM image recorded in a high-resolution, AMR scanning electron microscope.



Cr-Plated 105 mm

Bottom image: optical micrograph (reproduction of top panel, Fig. 7).

8. Fracture profiles and AES trace of 105 mm Cr-plated bore surface.



9. SEM/SAM analysis of fracture profile of 105 mm Cr-plated bore surface.